DROP IMPACT ON AN INCLINED AND MOVING SURFACE

SALMAN BUKSH SOOKRAN

A THESIS SUBMITTED TO

THE FACULTY OF GRADUATE STUDIES

IN PARTIAL FULFILLMENT OF THE REQUIREMENTS

FOR THE DEGREE OF

MASTER OF SCIENCE

GRADUATE PROGRAM IN MECHANICAL ENGINEERING

YORK UNIVERSITY

TORONTO, ONTARIO

AUGUST 2018

Abstract

This thesis has made progress in two different areas related to drop impact onto a surface. Firstly, a systematic experimental study has been performed to understand asymmetric spreading of low and high surface tension liquids on a moving surface. A new time evolution model for droplet spreading on a moving surface was developed. This model regardless the value of surface tension of the liquid can predict the spreading of low viscous (1-4cSt) liquids on a moving surface. Secondly, liquids with viscosity (1-5cSt) and surface tension (17.4-72.8mNm) were used to study the drop impact on moving and inclined surface. Experiments performed with similar normal (0.9-2.9m/s) and tangential (0.8-2.9m/s) velocities on both surfaces to test our hypothesis that spreading/splashing for these two surface conditions should be same. Results indicates that our hypothesis is true, except for some special conditions when, normal and tangential velocities are greater than the range of our analysis.

Acknowledgement

I would like to acknowledge and thank the following important people who have supported me throughout my Master's degree.

Firstly, I would like to express my gratitude to my supervisor Prof. Alidad Amirfazli, for his helpful guidance and support for past 2 years and replying to my numerous emails.

I would also like to thank Prof. Marco Marengo for his guidance during his visit at York University. In addition, I am grateful to Mr. Hamed Almohammadi for allowing me to use his data and helping me in writing technical discussion.

Finally, I would like to thank my family especially my parent Salina Begum and Imam Buksh for their love and support.

Table of Contents

List of Tables

List of Figures

Chapter 1

Introduction

1.1 Background

Drop impact onto a surface has fascinated many researchers since Worthington released his first paper in the late 19th century (1). Since then, researchers have looked at different aspects of drop impact until recently when researchers have turned their attention on droplet impacting on a moving or an oblique surface. Drop impact onto an oblique or moving surface has various applications in industries such as in ink-jet printing, where an electronic charging and a deflection system is used to break continuous inkjet into tiny micro droplets which impacts on a moving paper (2–5). Spray coating is very important on medical devices such as for catheter (6), or coating electronics to save from wear, corrosion or making protective layer on a target surface (7–9). In agriculture industries, where weed and pest control is important to maximize crop production (10–12). However, for most of the industries mentioned above either has a surface that is moving or a surface that is not horizontal.

When a drop impacts on a stationary surface it may spread, splash or rebound (13–16). The physical parameters such as impact velocity (17–20), liquid properties (surface tension, viscosity) (21–24), surface properties (wettability, roughness) (25–28) and surrounding air (29,30) can affect the outcomes of drop impact. There are different drop impact outcomes seen on a stationary surface: Droplet deposition, prompt splash, corona splash, receding breakup, partial rebound and rebound Figure 1.1 shows different drop impact outcomes. Depending on the Weber number ($We = \frac{\rho d v^2}{\sigma}$), Weber number is the

ratio of droplet inertia to surface tension, where ρ is liquid density, d is the droplet diameter, v is the impact velocity and σ is the surface tension of the liquid. When a droplet with a small normal velocity impacts onto a surface, it spreads smoothly onto the surface and makes a thin pancake-like sheet, eventually recoils back and deposits, known as deposition. When the droplet velocity is increased, tiny droplets can come out from the lamella, known as prompt splash. A further increase in the normal velocity can cause a thin sheet of lamella lifting off from the surface making crown-like shape, at the edge of the crown tiny droplets comes out, this is often known as Corona splash. While, receding break up happens, when a droplet breaks into small pieces during receding. During recoiling if a portion of the droplet jets out from the liquid while the other part stays on the surface, then it is known as partial rebounding; and if the entire droplet jumps off from the surface against gravity is known as complete rebound.

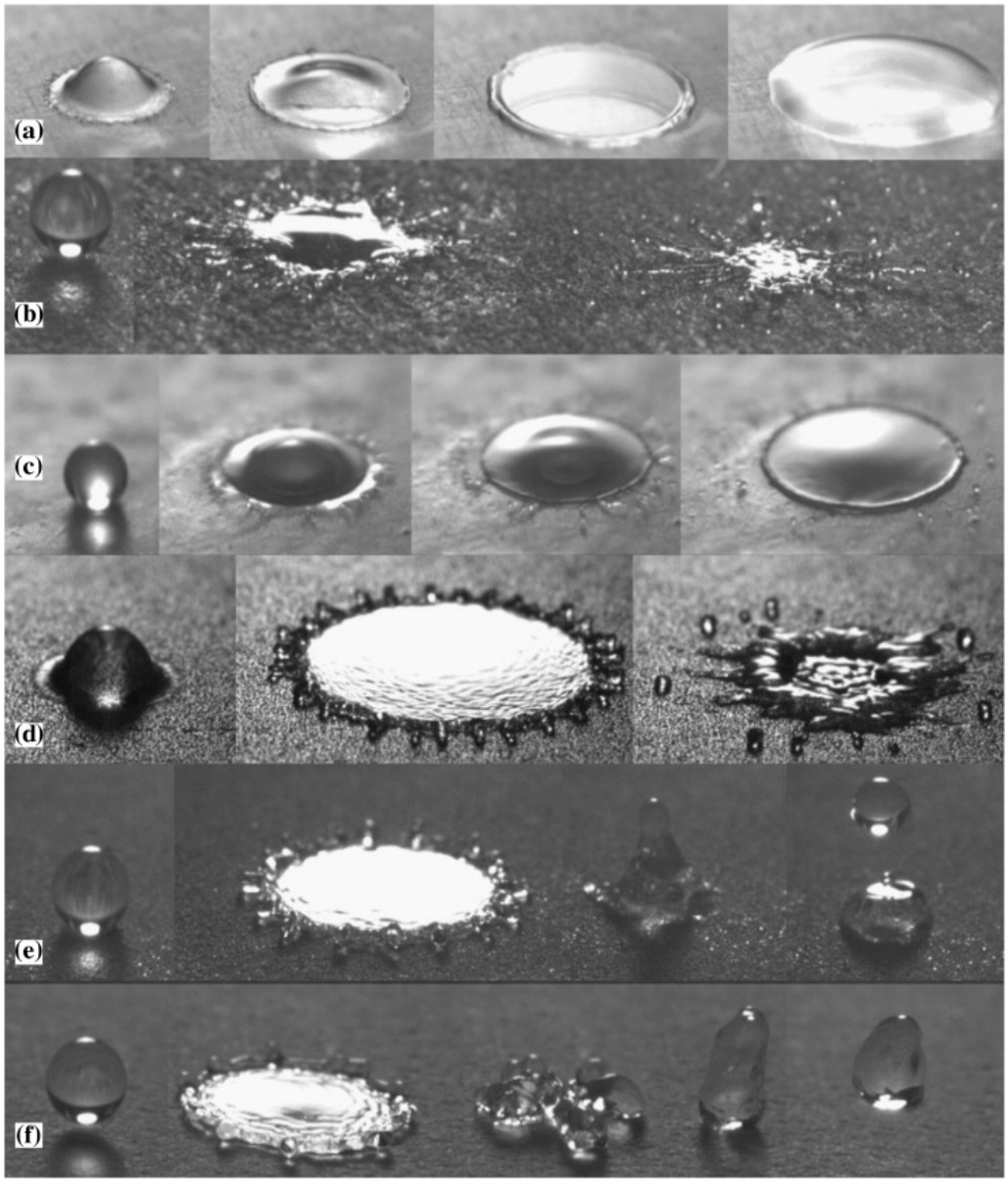

Figure 1.1 Outcomes of droplets on surface (a) droplet deposition; (b) Prompt splash; (c) Corona splash; (d) Receding break up; (e) partial rebound and (f) Complete rebound Reprinted from [Marengo M, Antonini C, Roisman IV, Tropea C. Drop collisions with simple and complex surfaces. Curr Opin Colloid Interface Sci. ***2011*** *Aug;16(4):292–302.] Copyright (2011), with permission from Elsevier.*

High surface tension and low surface tension liquids spreads differently on a stationary surface (31). Figure 1.2 shows that for same normal velocity of the droplet, high surface tension liquids reach its maximum width at an earlier time compared to low surface

tension liquids. Also, a high surface tension liquid has a smaller maximum width compared to a low surface tension liquid (32).

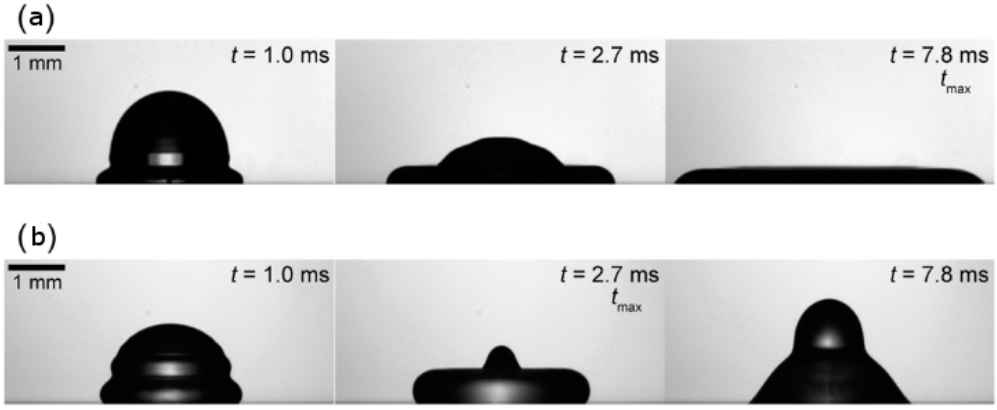

Figure 1.2 Spreading of (a) ethanol (low surface tension); (b) water (high surface tension) droplet on a stationary surface V_N= 0.5 m/s. Reprinted with permission from [Lee JB, Derome D, Guyer R, Carmeliet J. Modeling the Maximum Spreading of Liquid Droplets Impacting Wetting and Nonwetting Surfaces. Langmuir. ***2016*** *Feb 9;32(5):1299–308]. Copyright (2016) American Chemical Society.*

Drop impact on a surface has been researched both numerically and experimentally by many researchers. They have performed quantitative and qualitative analysis on the different droplet impact behavior on horizontal surfaces, such as effect of surface wettability, surface roughness or modeling the maximum width (31,33,34). However, in recent years researchers have focused their attention to drop impact onto inclined (35–41) or moving surfaces (29,42–46). For both inclined and moving surface, when a drop impacts along with a normal velocity component it also has a tangential or surface velocity component. One can think that if the velocities are kept same both surfaces can show same behavior. If so, it will be beneficial for others to replicate one conditions with other. However, a spreading lamella experiences different type of resistance on both of the surfaces, such as the flow of air above the moving surface or the tangential velocity on

inclined surface decreasing as drop spreads Figure 1.3. Also there are no validation literatures found which compares both of the conditions, so there is a need of research in this area.

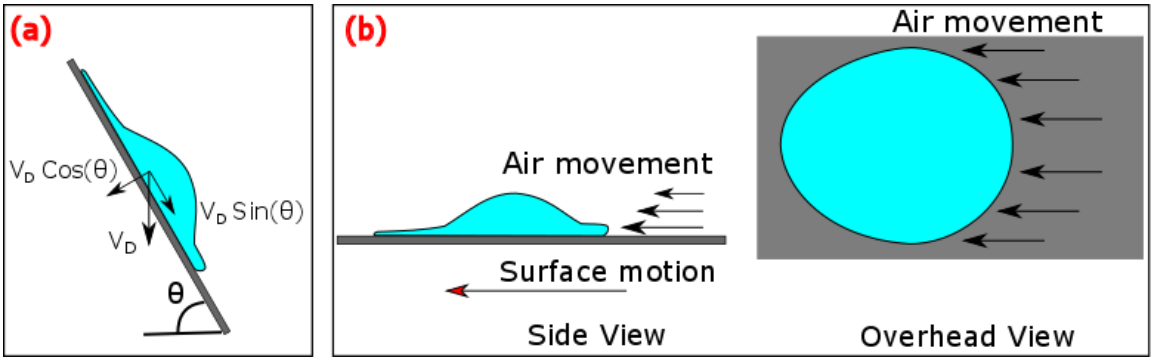

Figure 1.3 Schematic of droplet impacting on (a) inclined and (b) moving surface.

As mentioned above, researchers have mostly looked into how a droplet behaves upon impact over a moving surface or an inclined surface. For most of the cases they have observed the drop impact behavior such as (spreads or splashes). Sikalo et al. (41) used different types of liquids and surfaces to perform drop impact experiments on inclined surfaces. From their experimental results, they observed that droplet spreads, splashes or rebounds depending on the velocity and surface wettability. Bird et al. (35) developed the splashing threshold for ethanol on a moving surfaces, where they observed that increasing the surface velocity suppresses splashing at the back side of the lamella (region moving with the surface) we call this azimuthal splashing, this was also seen by other researchers (38,44).

However, on a moving surface overhead view images were used to show that a water droplet spreads asymmetrically along the direction of surface motion (43,46). It was also noticed that when the surface velocity is increased, a droplet splashes with an azimuthal angle over a moving surface, and the azimuthal angle also varies depending on the

surface velocity (44). Whereas, on an inclined surface, only Cui et al. (36) showed an asymmetric spreading of water however their research was only limited to droplet spreading. For rest of the studies on inclined surfaces only side view images were analyzed up to this date, thus the exact shape of the lamella cannot be determined. Also, the azimuthal splashing angle cannot be determined from the side view images.

As it can be seen that literatures for both inclined and moving surfaces show similar results (such as spreading or splashing). However, it is not clear, if the spreading of the lamella is same for both cases when the drop impact condition is identical; or if the splashing process is similar. Also, the literature mentioned here mostly performed experiments with high surface tension liquids (mostly water), and there are no studies found that studied the lamella propagation of low surface tension liquids on a moving surface. Therefore, it is not possible to say if the spreading of low surface tension liquids will be similar to high surface tension liquids in presence of surface velocity.

1.2 Objective of this thesis

Motivated by the previous works for both inclined and moving surface, a systematic study was performed to understand how a droplet behaves on both of the mentioned surfaces.

The objectives of this work were the following:

- Understanding the differences in spreading of low and high surface tension liquids
- Understanding the effect of surface velocity, surface tension over a spreading lamella and develop a universal spreading model.
- Comparing spreading results for similar conditions on inclined and moving surfaces with models from the previous literature
- Understanding the possible splashing seen on inclined and moving surfaces conditions and the effect of viscosity on drop splashing in presence of tangential velocity.

Experiments with different Newtonian liquids have been used to understand the droplet impact in presence of tangential velocity.

1.3 Thesis outline

This thesis is written by organizing two papers which are in the process of submission. Each chapter represents the work that will be presented in the paper. The manuscript for this thesis is structured below:

Chapter 2: We will study the spreading behavior of different low surface tension liquids on a moving surface. We will observe the effect of the droplet velocity and surface velocities for different low surface tension liquids. We will observe the lamella development for low surface tension liquids and compare with high surface tension liquids. Finally, we will develop an empirical spreading model which can predict the spreading of all types of liquids on moving surface, and validate the model with experimental results.

Chapter 3: We will perform experiments on inclined and moving surfaces with similar experimental conditions (i.e. normal and tangential velocity). We will use different types of liquids to see the droplet spreading and splashing on both inclined and moving surfaces. We will use hypothesis to confirm if spreading and splashing are similar in presence of tangential velocity, and use our model to further validate the results.

1.3.1 Direct Contribution

Given that this study is a continuation of the previous one, there has been some previous experimental set up that existed. Below I will provide information as which parts has been build up from ground up by me and which parts have been adopted or adapted by me. Furthermore, as this thesis is compilation of two papers to be submitted soon, I will also provide information below about role of each of the authors for the chapters.

Chapter 2: All the experiments have been performed by myself. I have used the stationary spreading data for high surface tension (24% wt. glycerol water and 42% wt. glycerol water) liquid from Hamed Almohammadi. He also helped me in constructing the spreading model and writing up in the discussion. Prof. Marengo and Prof. Amirfazli guided me to select the liquid and write the paper.

Chapter 3: I have performed all experiments, Prof. Marengo and Prof. Amirfazli guided write the paper.

Chapter 2

Spreading of low viscous liquids on a stationary and moving surface[1]

2.1 Introduction

Droplet spreading on a moving surface is frequently seen in applications such as inkjet–printing (2,3), agriculture (10,11), and spray coating (7,14). Most of the drop impact studies were focused on stationary surfaces, until recently when researchers turned their attention to drop impact on moving or inclined surfaces (where in both cases a droplet has a normal and tangential velocities relative to the surface) (35,37–39,41–44,46–50)

When a drop, with a given normal velocity (V_n) and diameter (D_o), impacts onto a stationary surface, the spreading takes places radially due to the initial kinetic energy of the droplet. The balance between kinetic energy, capillary, and viscous forces brings to the end of spreading process, and where the maximum lamella diameter D_{max} is seen at time t_{max} (26,51). Results from the literature (31,32,52) and also our own observations show the rate of spreading for low surface tension ($\sim 20\ mN/m$) liquids is different than that of a high surface tension ($\sim 70\ mN/m$) liquid for stationary surfaces (see Figure 2.1a, liquid properties are given in Table 1.1). The differences are due to the stronger capillary force for high surface tension liquids which modifies the form of the lamella with a larger rim, the larger rim causes a thicker viscous boundary layer (32) (see Fig. 8b in Ref. 32) which

[1] This chapter is to be submitted for publication soon. Authors: Salman Buksh, Hamed Almohhamadi, Marco Marengo and Alidad Amirfazli

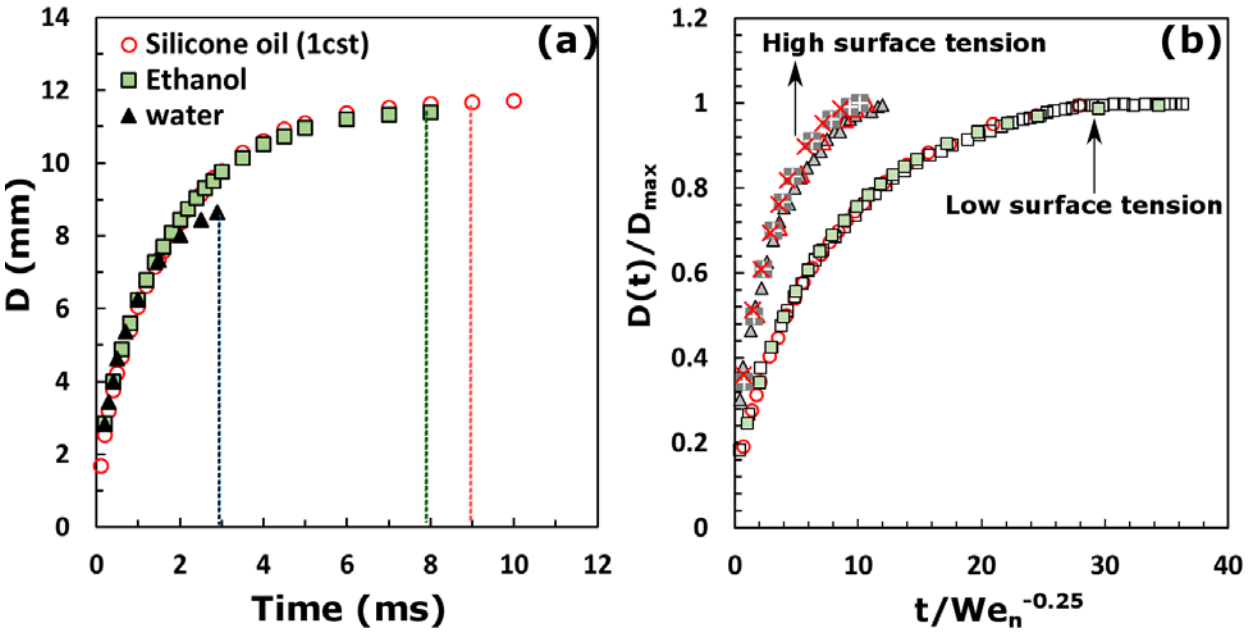

Figure 2.1 (a) Time evolution of the diameter of the lamella for impacting water, ethanol, and silicone oil (1cSt) droplets (V_n =1.6 m/s and D_o= 2.5 mm) onto a stationary hydrophilic (stainless steel) surface up to the maximum spreading. The dashed line denotes the t_{max}; (b) The nondimensionalized spreading factor for low and high surface tension liquids plotted against the scaled time on a stationary hydrophilic (stainless steel) surface. The impact conditions are: Unfilled square: ethanol, D_0= 2.7 mm, and V_n= 1.6 m/s; Unfilled circle: silicone oil (1cSt), D_0= 2.5 mm, and V_n= 1.2 m/s; filled triangle: water, D_0= 2mm, and V_n= 1m/s; filled square: ethanol, D_0= 1.8 mm, and V_n= 1m/s; unfilled triangle: water, D_0= 2.5 mm, and V_n= 3.4 m/s; positive: 2 cSt glycerol-water (2 cSt), D_0= 2.5 mm, and V_n= 2.5 m/s; cross: glycerol-water (4 cSt), D_0= 2.5 mm, and V_n= 2 m/s. The data shown with filled triangle and filled square are taken from Lee et al.(32) and unfilled triangle, positive, and cross are showing data from Almohammadi and Amirfazli[11]. In both references the studies surface is stainless steel.

Quantitatively, there are several spreading relation (27,33,51,53,54) in the literature that can predict the maximum diameter of a lamella. These relationships were developed using energy approach, momentum conservation bounding a rim, numerical solution of the Naiver Stokes equation, or scaling approach. To date, time evolution of spreading (i.e. D(t)) is quantified mainly using scaling approach due to the complexity of the matter. In this approach, the diameter of the lamella at a given time is normalized with the

maximum diameter ($D(t)/D_{max}$, also called spreading factor) and the time is scaled using $We^{-0.25}$ ($We = \rho V_n^2 D_0/\sigma$, the ratio of inertia to surface forces, where σ is the liquid surface tension and ρ is the liquid density) which is originally suggested by Clanet et al.(51). However, as it is clear in Figure 2.1b, using such scale, do not result in a universal curve (and subsequently relationship) when the data for liquids with various surfaces tensions are plotted together. This means that the Weber number alone cannot capture the effect of surface tension for droplet spreading and there is a need for rescaling. Note that as an initial approach for solving the problem, the power of Weber number was changed, but the spreading curve for low and high surface tension liquids could not be collapsed into a single curve.

Time evolution of a droplet spreading over a moving surface was studied only for high surface tension liquids (water and glycerin-water mixtures) (43,44,46). There are only two studies in the literature that considered low surface tension liquids, but they do not offer quantitative or even qualitative information about how a drop of low surface tension liquids spreads over a moving surface (the focus of these studies were on capturing splashing threshold) (35,45). When a drop impacts onto an inclined surface, or a surface that is moving in addition to the normal velocity with respect to the surface, the droplet also has a tangential velocity. In such cases, there are additional differences in the lamella spreading for low and high surface tension liquids. In the cases where there is a tangential velocity (i.e. moving surface), the spreading is symmetric only in the direction of surface motion (see Figure 2.2, where the yellow dashed line represents the line of symmetry). The lamella can be divided in two regions: the first region is the part of the droplet which moves against the tangential velocity, and to be consistent with the literature (43), we call

this region “upstream”, see Figure 2.2. The back side of the droplet that moves along with the surface (or tangential velocity) is called “downstream”. The delineation of two regions are at the maximum width position (shown with blue dashed line on Figure 2.2). The spreading of an impacting drop on a moving surface depends on several parameters such as: drop normal velocity, surface velocity (V_s), as well as the surface and liquid properties (43).

In this paper we will focus on spreading, so interested readers in splashing can refer to the literature (35,38,42,44). Figure 2.2 shows the spreading of water and silicone oil with the same viscosity of water (1cSt) on a moving surface at t_{max}. Note that since the spreading is not symmetric (unlike stationary surfaces) over a moving surface, the t_{max} is defined as a time when the lamella reaches its maximum width (W_{max}) in the perpendicular direction to the surface movement (or tangential velocity direction, see Figure 2.2). For water, the maximum width is relatively closer to the upstream side of the lamella compared to silicone oil, i.e. the length of the upstream over total length of the lamella is smaller. For instance, in Figure 2.2, such ratio (i.e. length of upstream over the length of lamella) is 0.37 for water and 0.46 for silicone oil (1cSt). Also, for silicone oil (1cSt) the area covered by the spreading lamella is larger compared to water for the same droplet velocity and volume (this is similar to drop impact onto a stationary surface). Furthermore, as for the moving surface, the t_{max} is higher for low surface tension liquids similar to a drop impact onto a stationary surface see Figure 2.1a.

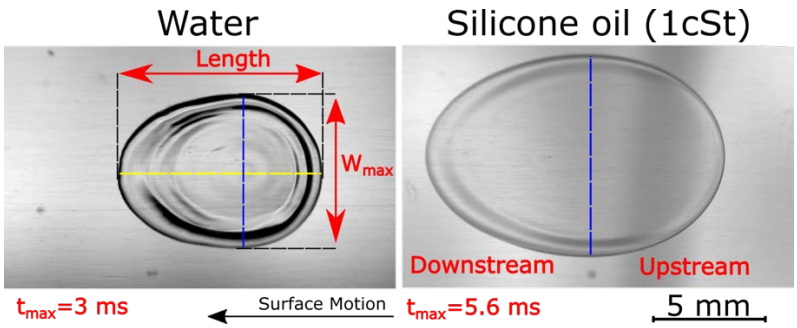

Figure 2.2 The maximum spreading of water and silicone oil droplets on a moving surface. Drop velocity, Vn = 1.20 m/s and surface velocity, Vs = 1.50 m/s, D_0= 2.5 mm

Collectively in the literature, there are some qualitative data for low surface tension liquids on stationary surface; however, there is no relation to predict the spreading of a droplet over a stationary surface for liquids with various surface tensions. Aside from this, in the case of moving surfaces, the literature does not have any quantitative/ qualitative data or any relationship which can predict the time evolution spreading of low surface tension liquids (35,41,45).

This study aims at understanding the spreading behavior of low surface tension liquids. This is important as many liquids used for inkjet printing (3) or in agriculture pesticides (12) have a low surface tension liquids that spreads on a moving or inclined surface. We present experimental data for low surface tension liquids, develop a spreading model which works for both stationary and moving surfaces, and validated the model against our experimental data.

2.2 Theoretical background for high surface tension liquids and moving surfaces

Our departure point will be an examination of drop impact onto a surface for high surface tension liquids. After a high surface tension liquid droplet touches the moving surface, it starts to spread radially at initial time. The radial spreading is seen due to the kinetic energy that generates a fast lamella velocity. Drop impact position (the point on a surface where the droplet touches at t=0 ms) moves towards the downstream region with surface velocity (see Figure 2.3a the white cross signifies the drop impact point). The liquid from the droplet bulk (see Figure 2.3a) comes down (due to the remaining inertia and gravity) in a forward position with respect to the drop falling point (blue line in Figure 2.3). As time progresses the droplet bulk moves further away from the impact point in the downstream region (see images at 0.5 ms and 3.0 ms in Figure 2.3*a*). After a certain time, the liquid from the droplet bulk cannot reach the downstream region anymore (see Figure A1 in the Appendix A, to see the lamella velocity at downstream region). Hence, the lamella velocity at the downstream region decreases and starts to move with the surface velocity, which distorts the circular shape of the spreading lamella (this is shown with a red circle in Figure 2.3*b* at t= 1.5ms the spreading lamella is not circular anymore). The droplet bulk disappears and the spreading lamella loses its kinetic energy gradually until its maximum width at t_{max}.

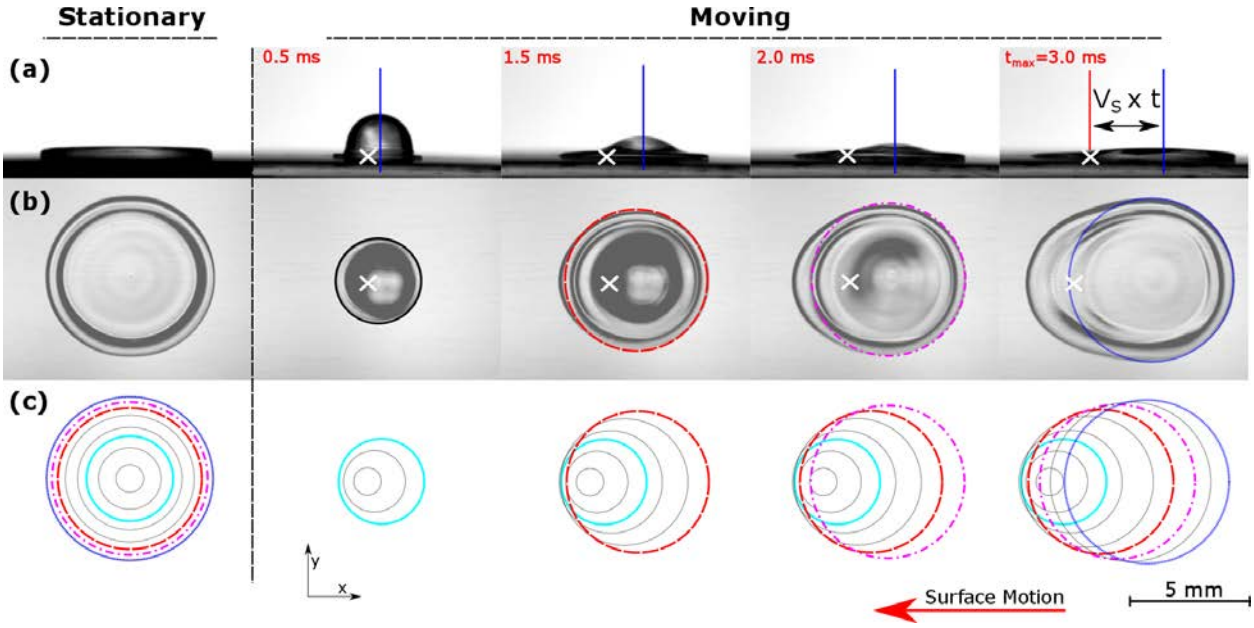

Figure 2.3 Time evolution for spreading of water droplet (V_n = 1.20 m/s and V_s = 1.50 m/s) on a moving surface; (a) side view images of a water droplet on a stainless steel (hydrophilic) moving surface, white cross refers to drop impact position, solid blue line refers to the drop falling path; (b) overhead view of water droplet; (c) time evolution of water droplet (up to t_{max}) and the model predictions(43) for V_n = 1.20 m/s and V_s = 1.50 m/s, the colored circles represents droplets at different time intervals where 0.5 ms (aqua), 1.5 ms (red), 2.0 ms (purple) and 3.0 (blue)

Almohammadi and Amirfazli (43) proposed a spreading model starting from the pictorial representation of the circles shown in Figure 2.3*c* on a stationary surface. The lamella outline at different time intervals is represented with different colored circles, with the size of the circles increasing as time progresses (spreading of lamella). They proposed a correlation for the spreading D(t) (we will extend this later in section 2.5) which can predict the lamella outline on a stationary surface. For the moving surface, they observed that if the circles (starting from the initial stationary position on the surface) are shifted in the direction against the surface motion (tangential velocity), the enveloping outline for the shifted circles is just as same as the lamella outline seen on a moving surface (43).

The shifting of circles against the direction of motion is given by x_{disp}:

$$x_{disp} = V_s\, t - C \quad (1)$$

where, the term $V_s\, t$ is the velocity of the center of the circle from its initial impacting point, and C is a shifting factor, i.e. the translation length of the local for the maximum width of the lamella, relative to the local of the droplet apex.(43) The term C is a time dependent variable which varies with the droplet normal velocity, surface velocity, and viscosity of the liquid. At any instant, then, the circles shown in Figure 2.3c, can be represented as:

$$y^2 + (x - x_{disp})^2 = r(t)^2 \quad (2)$$

where r(t) (=D(t)/2) is the lamella radius at a given time for a stationary surface.

When considering the above mathematical representation and from Figure 2.3c, one can notice that the model for drop impact onto a moving surface proposed by Almohammadi and Amirfazli (43) will always have the maximum width closer to the upstream region. However, for low surface tension liquids, we observed that the maximum width at t_{max} is closer to the centroid of the lamella (see Figure 2.2). This suggests that equation 2 needs to be modified to allow for constructing a model for spreading of low surface tension liquids, i.e the assumption of circles representing instantaneous spreading of the liquids shown in literature (43) is not suitable.

2.3 Methods and materials

The experiments were performed using a glass syringe generating water, ethanol, and silicone oil (1cSt) droplets. These liquids gave us a range of surface tension while keeping a similar value of the kinematic viscosity (ν), see Table 2.1. Droplet was allowed to fall

under gravity and the normal velocity was varied by changing the height between the needle and the surface. Droplet velocity was increased until splashing was observed for ethanol and silicone oil. Side view images at different time intervals were taken to measure the normal velocity of the droplet. The liquid properties as well as the advancing θ_A and receding θ_R contact angles are given in Table 2.1. Details about droplet velocity/ contact angle measurement can be seen Appendix C.

Images from top and side views were taken at 10,000 fps using Phantom Miro M320 (overhead view) and Phantom v 1610 (side view). Both cameras were synchronized and triggered instantly as the droplet was released. Each experiment was repeated 3 times, and the surface was cleaned with acetone and DI water before every experiment to remove remaining any liquids from the surface.

The experimental setup (Figure 2.4) consisted of 10 (180 mm X 20 mm) strips of stainless steel surface with roughness of 29 ± 2 nm mounted on a wheel (radius 284.5 mm). This gave a continuous horizontal moving surface with negligible curvature. The wheel velocity which was limited to 3 m/s (further increase led to splashing) and was operated using a TORQUEMASTER 4100 servo motor, and the wheel velocity was controlled using the software ROBORUN+. Before each experiment, the wheel velocity was set manually on the software and was checked using top view image to ensure its accuracy.

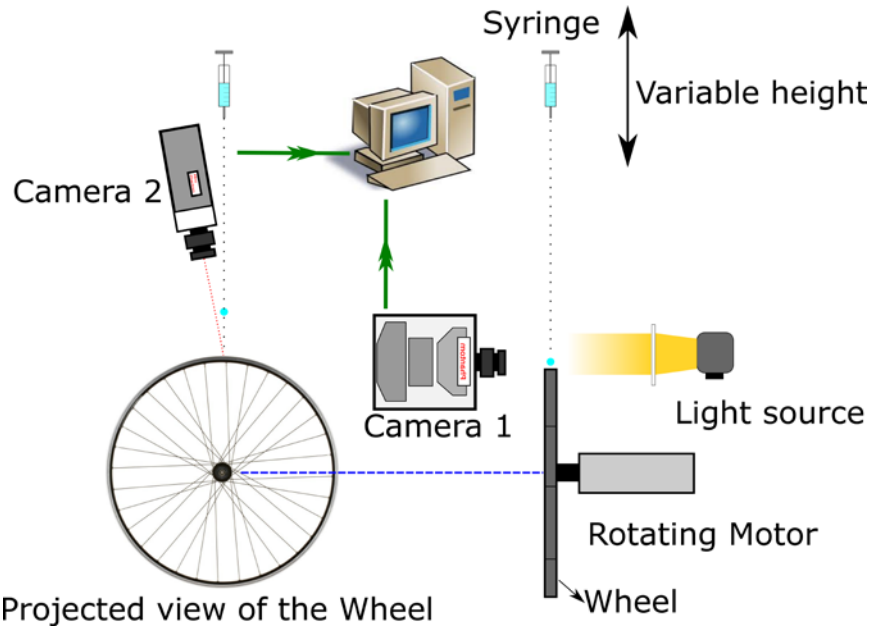

Figure 2.4 Schematic of the experimental setup for moving surfaces.

Table 2.1 Impact conditions and physical properties for test liquids

Liquids	D_0 (mm)	V_n (m/s)	ρ (kg/m^3)	ν (m^2/s)	σ(mN/m)	θ_A(°)	θ_R(°)
Water	2.5 ± 0.1	1.2-3.5	998 (42)	1.0 (42)	72.8 (42)	88° ± 2°	32° ± 2°
Ethanol	2.7 ± 0.1	0.9-1.7	786 (55)	1.52 (55)	23.2 (55)	<5°	<5°
1 cst Silicone oil	2.5 ± 0.1	1.0-1.7	818[a]	1.0[a]	17.4[a]	<5°	<5°
Glycerine-water(24% wt.) (44)	2.5 ± 0.1	0.8-2.5	1062	1.9	70.9	NA	NA
Glycerine-water(42% wt.) (44)	2.5 ± 0.1	0.8-2.1	1108.6	3.7	69.0	NA	NA

a) data has been taken from http://www.powerchemical.net/library/Silicone_Oil.pdf

2.4 Experimental results

From our experimental results we have noticed that spreading of low surface tension liquids can be divided into two parts: an initial phase, when the spreading is similar to high surface tension liquids; and a late phase, when the spreading is different compared to high surface tension liquids.

Initial phase. At an initial time on a moving surface, spreading of low surface tension liquid is similar to a high surface tension liquid. Right after the impact a circular spreading can be observed, due to the high initial kinetic energy of the droplet (see Figure 2.5a the yellow circle on third row at time 0.5 ms). As time progresses the circular spreading starts to change its form and the position of the maximum width of the lamella remains closer to the edge of the upstream region (see the yellow circle at t=2.5 ms on Figure 2.5a), similar to the case of a high surface tension liquid. The blue cross on the first row of Figure 2.5a shows the initial impact point of the droplet and the red vertical line shows the position of droplet apex. The results (Figure 2.5b) for different surface velocities shows that the distance between the droplet apex and the impact point is always equal to $V_s t$. The second row on Figure 5a shows the overhead image of silicone oil (1 cSt) droplet, and the blue dashed line shows the position of maximum width; it can be noticed that as time increases from 0.5 ms to 2.5 ms, the spacing between the two lines (blue and red) increases; this is captured by the shifting factor, C in Eq. 1.

Late phase. As time increases (till t_{max}), the position of the maximum width starts moving towards the center of the lamella. This can be seen by following the evolution of yellow circle on Figure 2.5a. The shape of the lamella becomes elliptical at the upstream region (unlike circular shape for high surface tension liquids see Figure 2.2 and ref.(43)). During

this time, we observed two changes in spreading: first, stretching of the lamella in the direction of motion (denoted with *a* on Figure 2.5a) and second, width-factor of lamella in the direction perpendicular to motion (denoted with *b* on Figure 2.5a). Note that spreading of width is lower compared to that of stationary surface at a given time thus we use the term “width-factor”. Our conjecture is that both stretching and width-factor of the lamella happens due to the kinetic energy of the lamella becoming less influential compared to the growing viscous boundary layer. Thus, the momentum transfer from the surface (which is function of the viscous boundary layer) to the lamella becomes more dominant. This in turn results in a shift of the lamella in the direction of the surface movement. Finally, the capillary force will become dominant over the remaining kinetic energy of the system which brings to an end of the spreading phase.

Stretching of lamella in the direction of the surface velocity vector (upstream) and width-factor in the direction of width occurs at same time, both phenomenon was noticed for all conditions where a tangential velocity was present. The stretching is observed because liquid closer to the surface starts moving with the surface velocity as described earlier. However, both phenomenon is not seen for high surface tension liquids because the lamella thickness is higher compared to low surface tension liquids, which means the viscous boundary layer thickness has minimal or no effect on high surface tension liquids during the spreading phase (32). From our experimental data we have noticed that the stretching and width-factor starts around 2.8 ms for all drop impact cases (see Figure 2.5c and 2.5d, all the data points start to diverge around 2.8 ms), and during this time the maximum width starts shifting towards the middle of the lamella as shown on the last row of Figure 2.5a. Both stretching and width-factor of the lamella depends on the surface

velocity, from Figure 2.5c and 2.5d, it can be seen that for V_s= 1.0 m/s, the stretching of the lamella takes place in a similar time for droplets with different normal velocities (see Figure A2 in the Appendix A for other normal velocity). So one can conclude by saying that surface velocity (or tangential velocity) is the most important factor in determining the shape of the lamella at late stage of spreading.

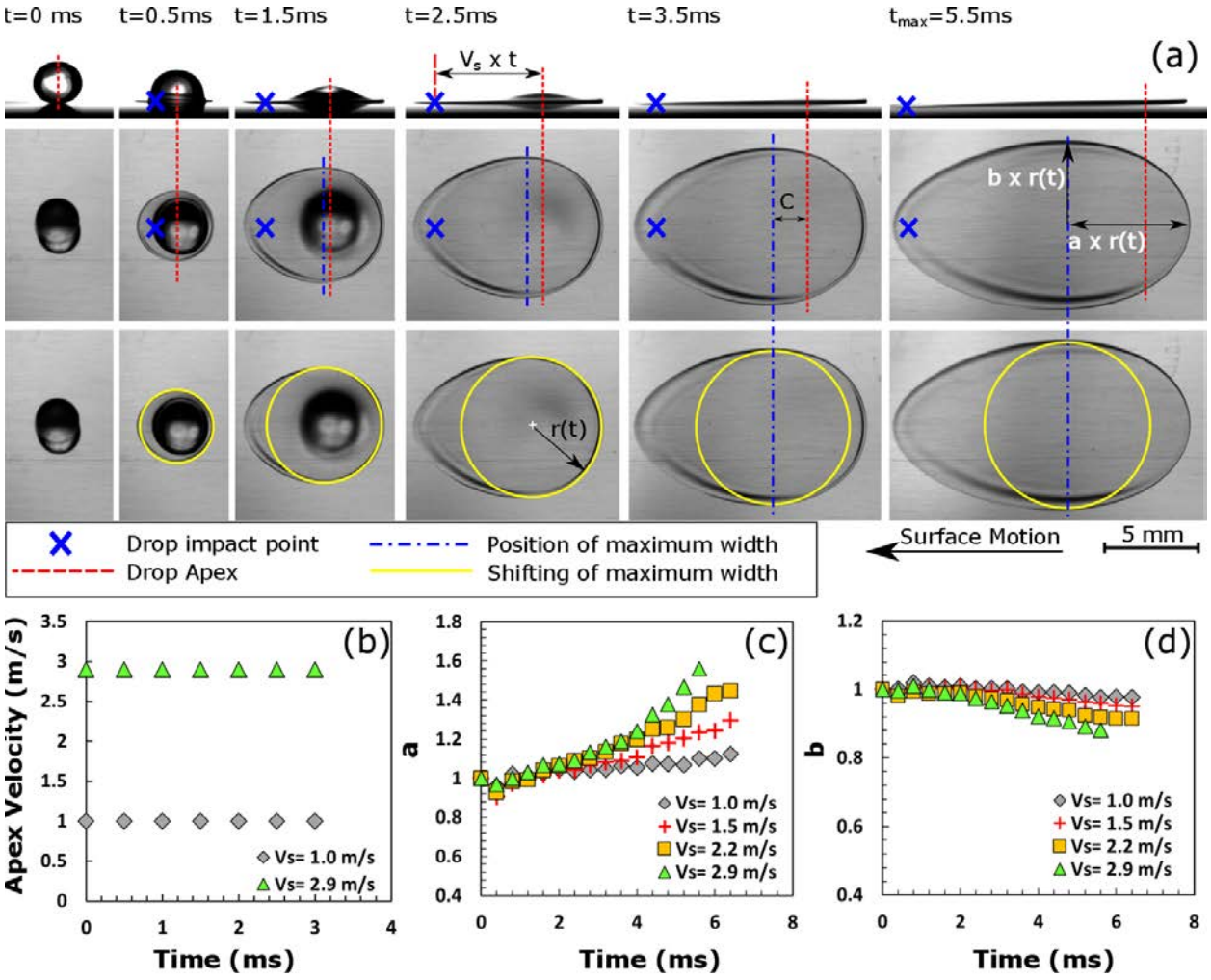

Figure 2.5 (a) Side and overhead view images for spreading of 1cSt viscosity silicone oil droplet (D_0=2.5 mm and V_n = 1.2 m/s) on a moving surface (V_s = 2.2 m/s). The blue cross denotes the impact point. The red dashed line represents the drop apex and the blue dashed line represents the position of maximum width. The solid yellow circle on the last row represents the shifting of maximum width on the surface. (b) Apex velocity with respect to time for V_n = 1.20 m/s at V_s = 1.00 m/s and 2.90 m/s. (c) The stretching of lamella in the direction of motion ***a(t)*** *normalized by r(t) for a stationary surface, at different time intervals, for V_n=1.0 m/s; and (d) Width-factor of lamella perpendicular to the direction of motion* ***b(t),*** *normalized by r(t) for a stationary surface, at different time intervals, for droplet impact conditions V_n=1.0 m/s and four different surface velocities, V_s=1.0 m/s (diamond), 1.5 m/s (cross), 2.2 m/s (square) and 2.9 m/s (triangle).*

2.4.1 Effect of impact and surface velocities on droplet spreading

Increase in droplet velocity (V_n), at a given condition, changes both the width and the length of the lamella. As the normal velocity of the droplet is increased, the maximum width becomes larger regardless of V_s, see Figure 2.6a. However, depending on V_s, an increase in V_n, the length of the lamella may decrease or increase on Figure 2.6b. Considering the slopes of trends shown in Figure 2.6a and 2.6b, an increase in drop velocity (V_n) results in a more rounded shape for the lamella, while the resultant lamella is more stretched for low V_n. The t_{max} decreases with V_n, see Figure 2.6d; so high droplet velocities (V_n) less time is available for the surface to stretch the lamella, and a rounded shape can be observed.

An increase in surface velocity influences the lamella shape as well. Figure 2.6c shows the normalized width at different times. With an increase in surface velocity, the width of the lamella becomes smaller compared to a lamella spreading over a surface having lower velocity (see V_s= 1.0 and 2.9 m/s on Figure 2.6c). This is also true at t_{max} where the maximum width of a spreading lamella decreases with an increasing of surface velocity, see Figure 2.6a. A similar behavior was also pointed out by Almohammadi and Amirfazli (43). In term of the length, lamella has higher length when the surface velocity is higher (see Figure 2.6b). Therefore, unlike the drop velocity (V_n), an increase in surface velocity (V_s) results in a more stretched shape for the lamella, while the lamella has more rounded shape when surface velocity is lower. This happens as the higher surface velocity does not allow enough time for the droplet bulk to release the liquid in the normal direction to surface velocity vector as it shift the available liquid toward downstream region.

Therefore, the length of the lamella at t_{max} is always larger when the surface velocity is increased.

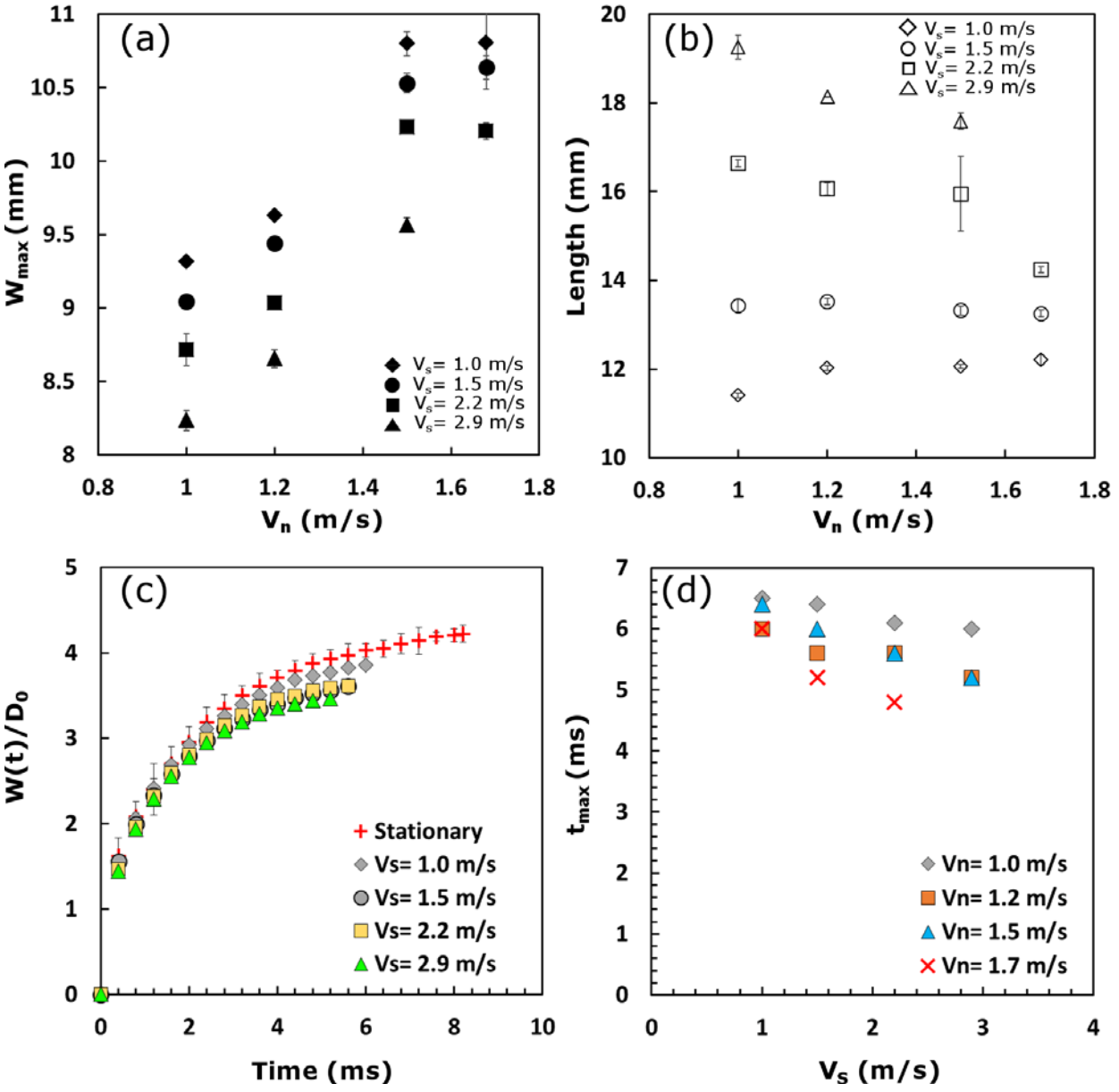

Figure 2.6 (a) W_{max} (solid), and (b) Length (unfilled) of the lamella at t_{max} for Silicone oil (1 cSt) droplet (D_0= 2.5 mm) at different normal velocities: 1.0 m/s-1.7 m/s, and surface velocities 1.0 m/s (diamond), 1.5 m/s (circle), 2.2 m/s (square), and 2.9 m/s (triangle). (c) normalized width plotted against time for V_n= 1.2 m/s for stationary surface and with different surface velocities. (d) t_{max} for different normal and surface velocities.

2.5 Model development for droplet spreading

In the previous section, our experimental results showed that there are noticeable differences in the spreading of low and high surface tension liquids on a moving surface (e.g. spreading time, spreading factor and the position of maximum width). From Figure 2.1b it was seen that the spreading ratio on a stationary surface for low and high surface tension liquids are different. Also our discussion from Section 2.4.1 showed that the behavior of low surface tension liquids starts to deviate from high surface tension liquids at about 2.8 ms. According to equation 2, which was developed for high surface tension liquids, a droplet on a moving surface will have the maximum width near the upstream region (due to semi-circle shape of the upstream region). Therefore, Equation 2 can predict the initial spreading, but it cannot predict the lamella outline for low surface tension liquids for a late time. As such there is a need for a modify the spreading model from Ref.(43)

To develop a spreading model for low surface tension liquids on a moving surface, r(t) is an important factor; hence, we will find the empirical correlation for r(t) first and use it to develop the model of spreading on a moving surface in next section. Following the idea from Almohammadi and Amirfazli (43) we will start by considering drop impact on a stationary surface first.

Spreading equation on a stationary surface. By introducing a surface tension term in the scaled time (i.e. $t/We^{0.25}$) as a ratio of liquid to water surface tension $(\frac{\sigma_L}{\sigma_W})^a$, all the data (Figure 2.1b) from literature (43) and from our experiments collapse into a single curve (see Figure 2.7 with all the data points). Note that at initial time the spreading factor

is zero and as it reaches to D_{max} the factor is 1. Therefore, to find an equation that can find spreading factor on a hydrophilic surface, we should consider two issues: first, the correlation should predict zero when time is zero; and secondly, it should be able to predict the r/r_{max} (or D/D_{max}) for other time intervals. Considering discussion above, we fit all our data (both low and high surface tension liquids) using the cftool in MATLAB and hence we define r(t) in the following form:

$$\frac{D(t)}{\mathrm{D}_{max}} = 1 - \exp(a(t\, We^{0.25}(\frac{\sigma_L}{\sigma_W})^{0.75})^b) \quad (3)$$

Here, t (ms) is the given time, *a* and *b* are the curve fitting coefficients; with values of a = -0.6000 and b= 0.7798 with an R^2 = 0.9848 and SSE = 0.2905. Equation 3 gives the spreading factor which can be used to find the radius or width of the lamella for a given time for liquids of any surface tension.

Since the model is based on circles (circular spreading at different time interval on stationary surface as mentioned before on Section 2.2), we decided to use the radius $r(t) = \frac{D(t)}{2}$ term in the equations from now for simplicity. Note that's spreading data for low and high surface tension (from Almohammadi and Amirfazli) fluids were also used to perform the curve fitting equation 3.

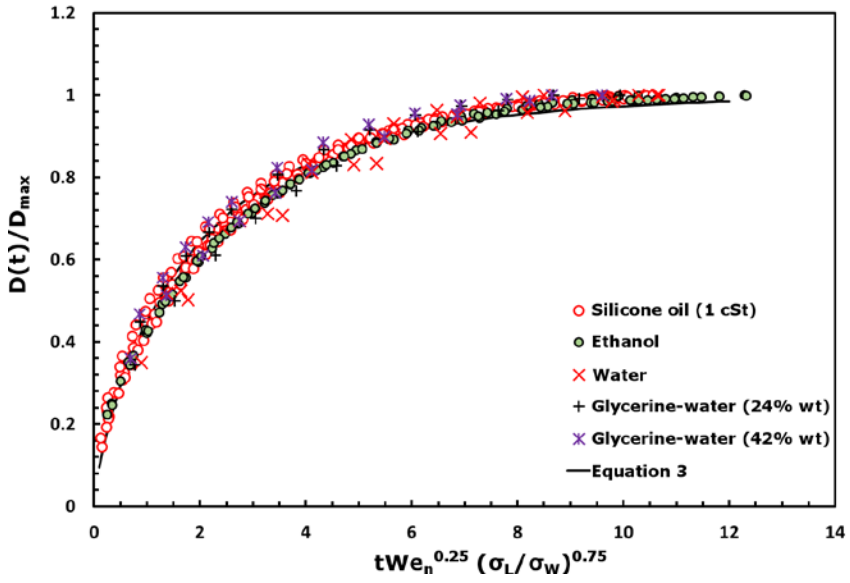

Figure 2.7 The nondimensionalised spreading factor of low and high surface tension liquids plotted against the scaled time fitted with new empirical model. The Eq. 3 represents the data well.

To remodel lamella on a moving surface, needs to generate a circular lamella outline at initial time and change it to ellipse as time progresses. This is so to capture the evolution of lamella over time as described earlier. According to our observations each circle/ellipse represents the outline of the lamella position at a snapshot of time in isolation.

The overall lamella outline at a certain time can be found when an enveloping line is drawn to encompass all the circles/ellipses, however one must remember that the enveloping line should have an egg/ellipse shape, see the white ellipse on Figure 2.8b at t=5.2ms.

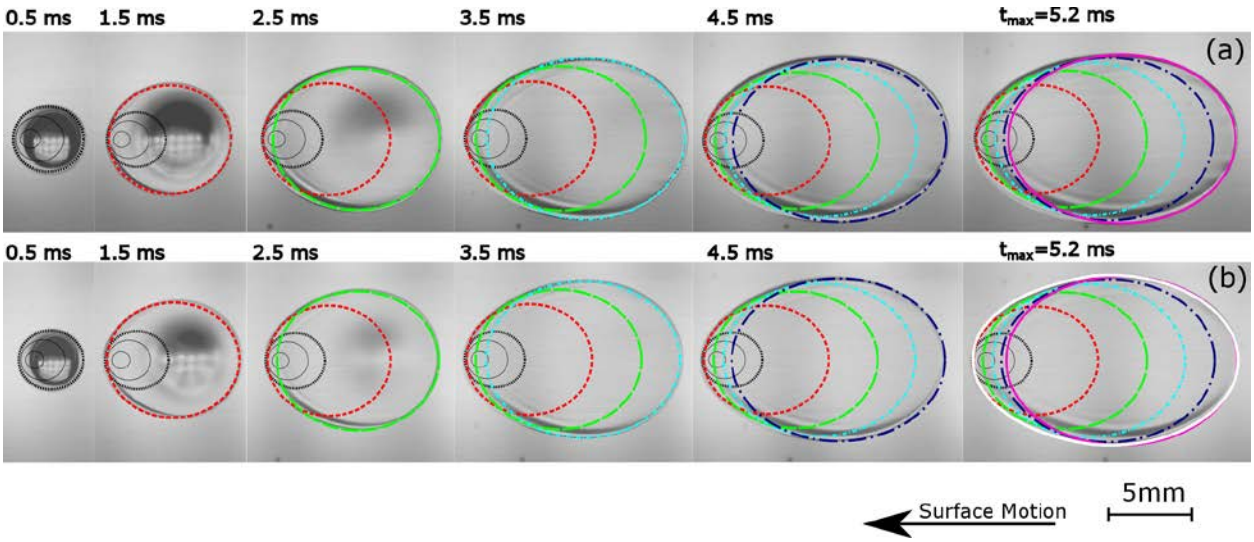

Figure 2.8 Spreading of (a) ethanol droplet with D0 =2.7 mm; (b) silicone oil (1 cSt) with D0=2.5 mm droplets at different time interval on a moving surface: Vn = 1.50 m/s and Vs = 2.20 m/s. Different coloured contours represent spreading of droplet at different time interval; and a white enveloping line over all the circles/ellipses shows the lamella shape.

Spreading equation on a moving surface. We start with the equation of a circle $\frac{x^2}{r(t)^2} + \frac{y^2}{r(t)^2} = 1$ where *r(t)* is the radius of the circle. It was seen that the stretching takes place in the direction of the surface motion (x direction with the factor *a*) and width-factor in the Y direction is represented with *b*. If we introduce these width-factor and stretching factors, the equation of circle changes to an ellipse as:

$$\frac{x^2}{(a \times r(t))^2} + \frac{y^2}{(b \times r(t))^2} = 1 \qquad (4)$$

The new spreading model will start as a circle and eventually it will become elliptical as time progresses (note ta and b are functions of time). Therefore, equation 4 can be re-written to a form that is similar to an equation of a circle, thus we can write following:

$$\frac{x^2}{a(t)^2} + \frac{y^2}{b(t)^2} = r(t)^2 \qquad (5)$$

There are three parameters in this equation which controls the spreading on a moving surface, coefficient $\boldsymbol{a}(\boldsymbol{t})\ and\ \boldsymbol{b}(\boldsymbol{t})$, depends on the drop impact condition and liquid parameters. The value for both ***a*** and ***b*** were found using our experimental data (see supplementary information for details). The other parameter is the shifting factor ***C,*** hidden in the x_{disp}(equation 1) i.e. the movement of the maximum width relative to the droplet apex, also calculated with fitting our experimental results (see supplementary information for details). Lamella propagation at different times was denoted as r(t) which can be calculated using equation 3.

According Almohammadi and Amirfazli (43), tangent to all the lines can be used to calculate the area of the enveloping line. Therefore, equation 5 and the derivative for equation 5 can be solved to to find the tangent.

$$\frac{d}{dt}\left[\frac{x^2}{a(t)^2}+\frac{y^2}{b(t)^2}=r(t)^2\right] \quad (6)$$

The resultant solution will be noted as $f_{tangent}\ (x,y)$

Now having the solution for all the tangent, the area of the lamella can be calculated by integrating $f_{tangent}\ (x,y)$, This will give the area of an enclosed lamella at any given time.

The new model (equation 5) can easily predict the spreading of both low and high surface tension liquids. However, one must always remember that the model can predict the shape of liquid only until t_{max}.

The new spreading model is applied on different droplet conditions. Figure 2.9 shows our new model compared to our experimental results. By accumulation of all the ellipses and

by drawing an enveloping contour, the model can predict the lamella shape at different time interval for different impact and surface velocities for silicone oil (1 cSt) and ethanol.

The model developed above also can predict the shape of high surface tension liquids too. Figure 2.10 shows the model can predict the spreading for water droplet on a moving surface. This proves that our model can predict the spreading of both low and high surface tension liquids on a moving surface.

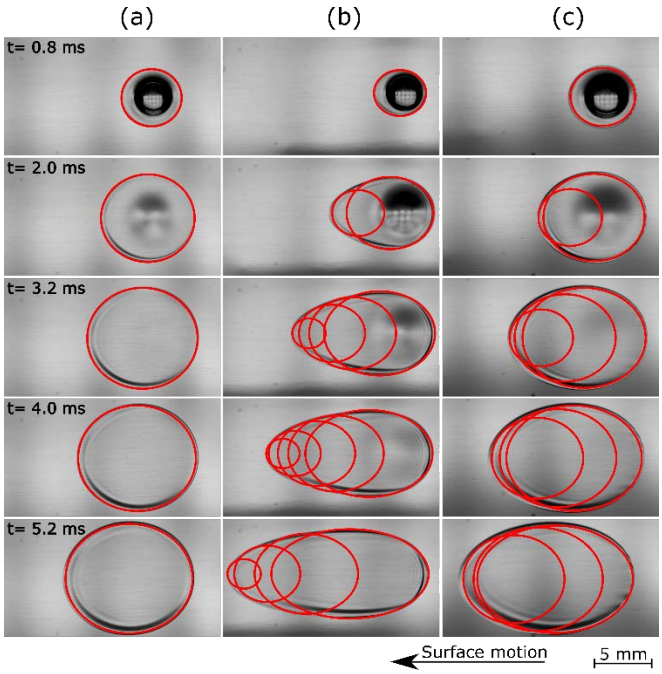

Figure 2.9 Applying the spreading model equation 5 for low surface tension liquids (a) silicone oil V_n= 1.50 m/s V_s =1.00 m/s, (b) silicone oil V_n = 1.00 m/s V_s =2.90 m/s; (c) ethanol V_n =1.50 m/s and V_s =2.20 m/s.

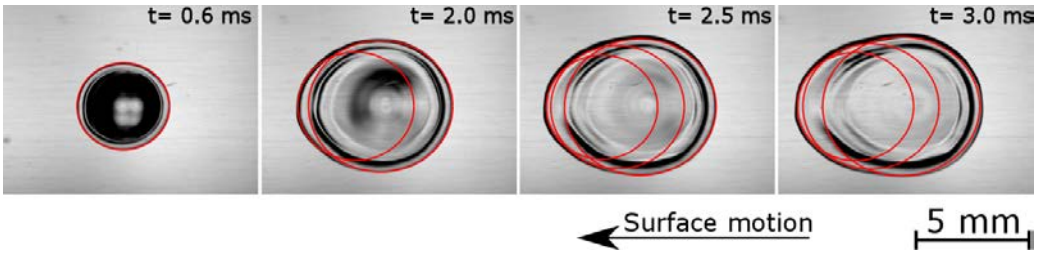

Figure 2.10 Spreading model applied on water droplets spreading on a moving surface D_0= 2.5 mm V_n= 1.20 m/s and V_s =1.50 m/s.

The model proposed here in this paper is valid for liquid viscosity upto 4cSt. This limitation has been also reported by Almohammadi and Amirfazli (43). Above 4 cSt, the viscosity of the liquids strongly influence the spreading of droplet, hence the empirical scaling (51) $We^{0.25}$ cannot be used anymore.

Chapter 3

Impacting of droplets on moving surface and inclined surfaces[2]

3.1 Introduction

Droplet impacting on a surface can be widely seen in different industrial applications such as inkjet printing (2,3), spray coating (7,56) and in agriculture (10,11). In these applications most of the time either the surface is moving, inclined, or the combination of both. In recent years, there are a few works that have focused on drop impact onto a moving surface (42–47) or on inclined surface (35,37–39,41,49,57–59); experiments with various liquids i.e. low and high surface tension liquids with low and high viscosities are done. However, for both surfaces, most of the literatures generally examines droplet impact behavior (spreading, splashing or rebound), or mainly focused on capturing the splashing threshold. For both moving and inclined surfaces, the presence of tangential (or surface) velocity changes the behavior of a spreading lamella compared to a stationary surface.

On a horizontal surface, a droplet after impact will spread or splash radially depending on the Weber ($We = \frac{\rho\, d v^2}{\sigma}$) number of the liquid; where ρ is the density of liquid in kg/m^3, d is the diameter of the droplet, v is the normal droplet velocity and σ is the surface tension of the liquid. The outcomes of drop impact may also vary depending on the liquid viscosity (44,60,61), surface roughness (30,60) and surrounding gas pressure (18,29). When the We is increased, a spreading lamella will have a larger diameter and the time to reach

[2] This chapter is to be submitted for publication soon. Authors: Salman Buksh, Marco Marengo and Alidad Amirfazli

the maximum width (for lamella) becomes smaller (54). Increase in We will eventually change spreading to prompt splashing; a prompt splash is a type of splash where the kinetic energy stored in the liquid droplet allows some satellite droplets to eject from the advancing contact line of a spreading lamella. Further increase in the We leads to a corona splash, where the lamella lifts off from the surface and makes a crown shape before satellite droplets detaches from the rim of the crown.

On an inclined surface, when a droplet impacts with a velocity $V_{D,}$ the velocity will have two components: Normal velocity ($V_n = V_D\, cos\,(\theta)$) and tangential velocity ($V_t = V_D\, sin\,(\theta)$). For a moving surface, the velocity of the droplet driven by gravity is called the normal velocity V_n, and the tangential velocity can is the velocity of the surface, V_s . In the presence of tangential velocity, the lamella will not be symmetric unlike the case for drop impact onto a horizontal stationary surface. For cases where a tangential velocity is present, the spreading lamella can be divided into two regions. The first region is the part of the droplet which moves against the surface (or moves down the plane for inclined surface) to be consistent with the literature, we call this region “upstream”. The back side of the droplet that moves with the surface (or moves against the gravity for inclined surface) is called “downstream”; and delineation for the regions is the position of the maximum width of lamella (as observed normal to the direction of tangential velocity on the plane of the surface), see Figure 3.1.

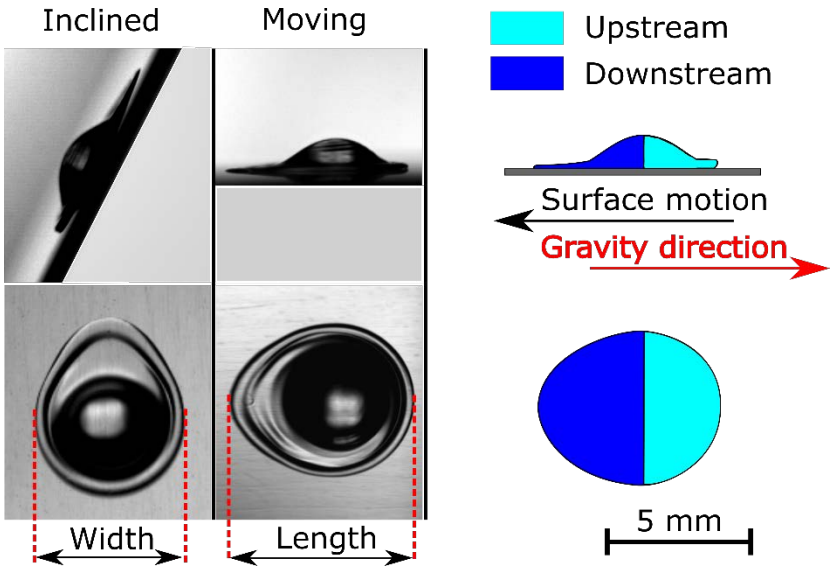

Figure 3.1 Showing the schematic and images of droplet spreading on a moving and inclined surfaces.

In presence of a tangential velocity, different spreading behavior is seen. At initial time, right after impact, droplet will spread radially (i.e. symmetrically), this is mainly due to the high kinetic energy stored on the droplet. As time progresses, the kinetic energy on the spreading lamella decreases and the tangential/surface velocity affects the spreading lamella, which changes the circular shape of the lamella to an egg or oval shape. Tangential velocity has a very important role on the spreading lamella, with an increase in tangential velocity, the spreading lamella will have a longer length (i.e. lamella length parallel to the direction of surface motion/ tangential velocity see Figure 3.1). However, further increase in tangential velocity can lead to an azimuthal splashing (see Figure 3.2a), where the spreading take place at the downstream region and the upstream region splashes to the extent of an azimuthal angle, φ. On the other hand, if the normal velocity is increased, an all-around (360° splash Figure 3b) axisymmetric splashing is seen. Almohammadi and Amirfazli (44) proposed X-Y convention to explain different types of splashing, where, X denotes the downstream region of the droplet and Y denotes the

upstream part of the droplet. They identified four types of splashing spreading prompt, spreading corona, prompt corona and asymmetric corona splash (this will be discussed later in chapter 3.3.2).

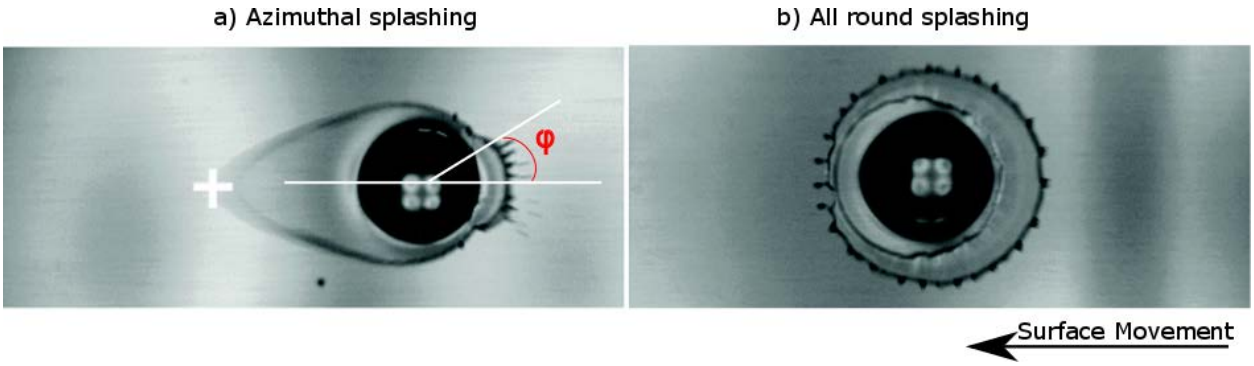

Figure 3.2 Different splashes seen on a moving surfaces (a) Azimuthal splashing V_n= 2.90 m/s V_t= 14.9 m/s; (b) All round splashing V_n= 3.2 m/s V_t= 1.5 m/s. The white cross refers to the point of impact, and φ represents the azimuthal splashing angle. Reprinted with permission from [Almohammadi, H. & Amirfazli, A. Understanding the drop impact on moving hydrophilic and hydrophobic surfaces. Soft Matter ***13,*** *2040–2053 (2017).]. Copyright (2017) Royal Society of Chemistry.*

Most of the works in the past have used side view images, however, for characterization of different splashing behavior, overhead view is very important for azimuthal splashing. Almohammadi and Amirfazli (44) showed that the azimuthal splashing angle varies with slight deviation in the normal and tangential velocity components, this information cannot be gathered from side view images. Therefore, it is essential to observe the behaviors from the overhead view.

For both cases, resistance from the surrounding can also affect the impacting droplet, such as, gravity can affect the tangential component of an inclined surface causing difference in the spreading of droplet. Also for a moving surface, air above the surface may create drag forces on the spreading lamella and cause difference on both

spreading/splashing behavior (see Figure 1.3). However, from literature it is not clear, if the droplet behavior upon impact to inclined and moving surfaces are identical. There is no concrete evidence in the literature to prove or disprove the preceding statement either in the form of experimental or numerical work in identical conditions. In this Chapter, we report on results from a series of systematic experiments with liquids of different viscosities and surface tension. We will use our results to quantify if drop spreading and splashing are similar or different for two systems of moving and inclined surfaces by using hypotheses.

3.2. Methodology and experimental setup

The experimental setup in Figure 3.3 consisted of a glass syringe to generate droplets of water, glycerol-water mixture and silicone oil droplets. The liquids chosen for the experiments have a wider range of surface tension (17.4~72.8 mNm) and viscosity (1~5 cst) see Table 3.1. Drop impact experiments were initially performed on inclined surfaces. Where the drop normal velocity was adjusted by changing the height between the needle and the surface. Normal and tangential velocities were changed by varying the angle of inclination of the surface with respect to horizon from 25° to 65°. Side view images were used to measure the component of normal and tangential velocities; and both velocities were replicated on a moving surface. Where normal velocity was changed by adjusting the syringe height and tangential velocity was changed by controlling the surface motion. The maximum velocity difference between two conditions were ± 0.05 m/s for either V_t or V_n.

Images from top and side views were taken at 10,000 fps using a Phantom Miro M320 (overhead view) and a Phantom v 1610 (side view). Both cameras were synchronized

and triggered instantly as the droplet was released. Each experiment has been repeated 3 times, and the surface was cleaned with acetone and DI water before every experiment to remove remaining liquids from the surface.

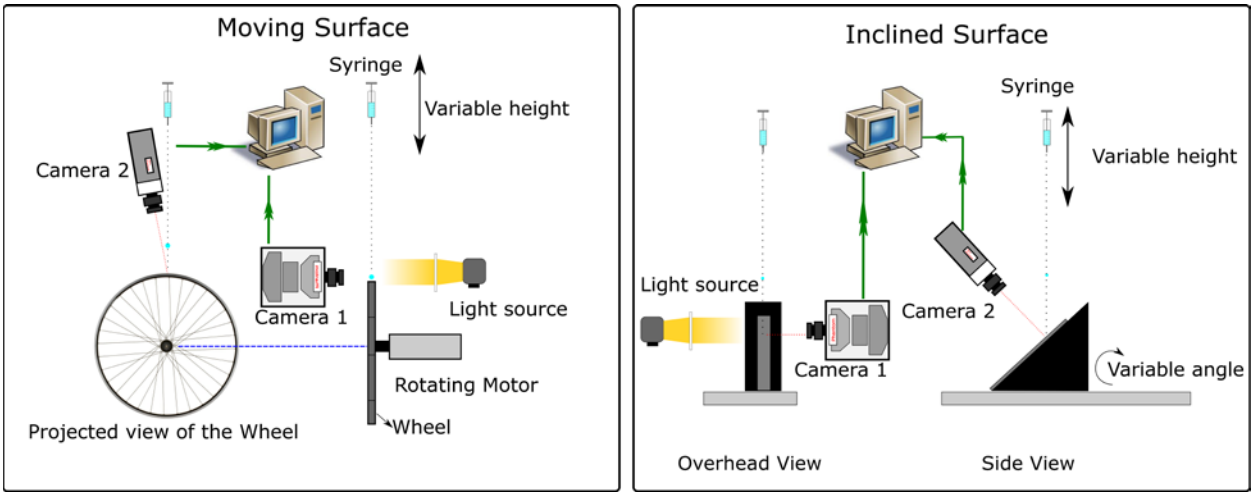

Figure 3.3 Schematic of the experimental setup for moving and inclined surfaces

For both setups the same stainless steel surfaces with roughness of 29±2 nm were used. The experimental setup for the inclined surface consisted of a stainless steel surface, a 3D printed surface holder with slots at (25°- 65°) to keep the angle of inclination constant. For the moving surface, the setup consisted of 10 (180 mm X 20 mm) strips of stainless steel surface mounted on a bicycle wheel (radius 284.5 mm). The wheel was attached to a servo motor whose velocity was controlled using the software ROBORUN+.

Table 3 1 Properties of liquids used, range of velocities studied and the wettability of surface with test liquids

Liquids	D_0 (mm)	Normal Velocity (m/s)	Tangential Velocity (m/s)	Density (kg/m^3)	Kinematic viscosity (m^2/s)	Surface tension (mN/m)	θ_A	θ_R
Water	2.5 ± 0.1	1.2-2.9	1.2-2.9	998 (42)	1.0 (42)	72.8 (42)	88° ± 2°	32° ± 2°
Glycerin-water(40% vol)[b]	2.6 ± 0.1	1.2-2.9	1.1-2.7	1104.4 (62)	4.37 (63)	69.8 (62)	82° ± 3°	45° ± 3°
Silicone oil (1 cSt)	2.5 ± 0.1	1.0-2.4	1.0-2.4	818[a]	1.0[a]	17.4[a]	<5°	<5°
Silicone oil (5 cSt)	2.5 ± 0.1	0.4-2.4	0.6-2.4	918[a]	5.0[a]	17.4[a]	<5°	<5°

a) data has been taken from http://www.powerchemical.net/library/Silicone_Oil.pdf

b) at 21.5° C

For droplet spreading we started analyzing our results from initial impact until the maximum spreading of the droplet was seen, which varies from 3 ms (for high surface tension liquids) to 7 ms (low surface tension liquids).

3.3. Results

The results will be presented in terms of spreading and splashing. In the first part we will compare the spreading results on a moving and inclined surfaces for all liquids. Next, splashing for liquids except water will be discussed; the We for water could not be increased to a value that a splashing can be observed.

Hypothesis development

Impacting of droplet on an inclined and moving surface generally has two different outcomes spreading and splashing. To compare the result for inclined and moving surfaces, we propose hypotheses to analyze our results. The hypotheses are as follows:

For spreading, at first we state that, length and width are similar on inclined and moving surfaces. Secondly, the lamella propagation should be same for both cases, from initial time of impact until maximum width is reached (i.e. are the shape similar for both cases).

For splashing, at first, the behavior should be similar for both surfaces i.e. if azimuthal or all-around splashes seen for same condition. Secondly, the azimuthal splashing angle, φ should also be similar quantitatively for both cases.

3.3.1 Spreading

When a droplet impacts on a moving/ inclined surface, a radial spreading is seen, see red circle on Figure 3.4a and 3.4b. Our experimental data on Figure 3.5c shows the width and length at initial time are same, which confirms the radial spreading. The spreading is radial, because the lamella velocity at initial time is higher (due to high kinetic energy) than the tangential velocity, therefore the spreading lamella retains a circular shape. However, as time progresses, the lamella velocity decreases and the tangential velocity starts effecting the spreading lamella, causing the radial spreading to change. Low surface tension liquid spreads differently on a moving surface compared to high surface tension liquids. On a moving surface, high surface tension liquids, at t_{max}, the spreading lamella makes an egg shape and its maximum width is seen near upstream region (43,44,46). Whereas, for low surface tension liquids, the spreading lamella makes an

elliptical shape. Our experimental results for water (high surface tension) and silicone oil (1cSt) (low surface tension) shows similar spreading on both inclined and moving surfaces (see Figure 3.4 *a* and *b*).

High viscous liquids also spreads radially at initial time after impact (see appendix Figure B1 *c* for our experimental data), and also the spreading behavior on an inclined and moving surface are similar. Figure 3.4 *c* shows that silicone oil (5 cSt) makes an elliptical shape and 40% glycerol water makes an egg shape as it approaches near t_{max} on Figure 3.4 *d*.

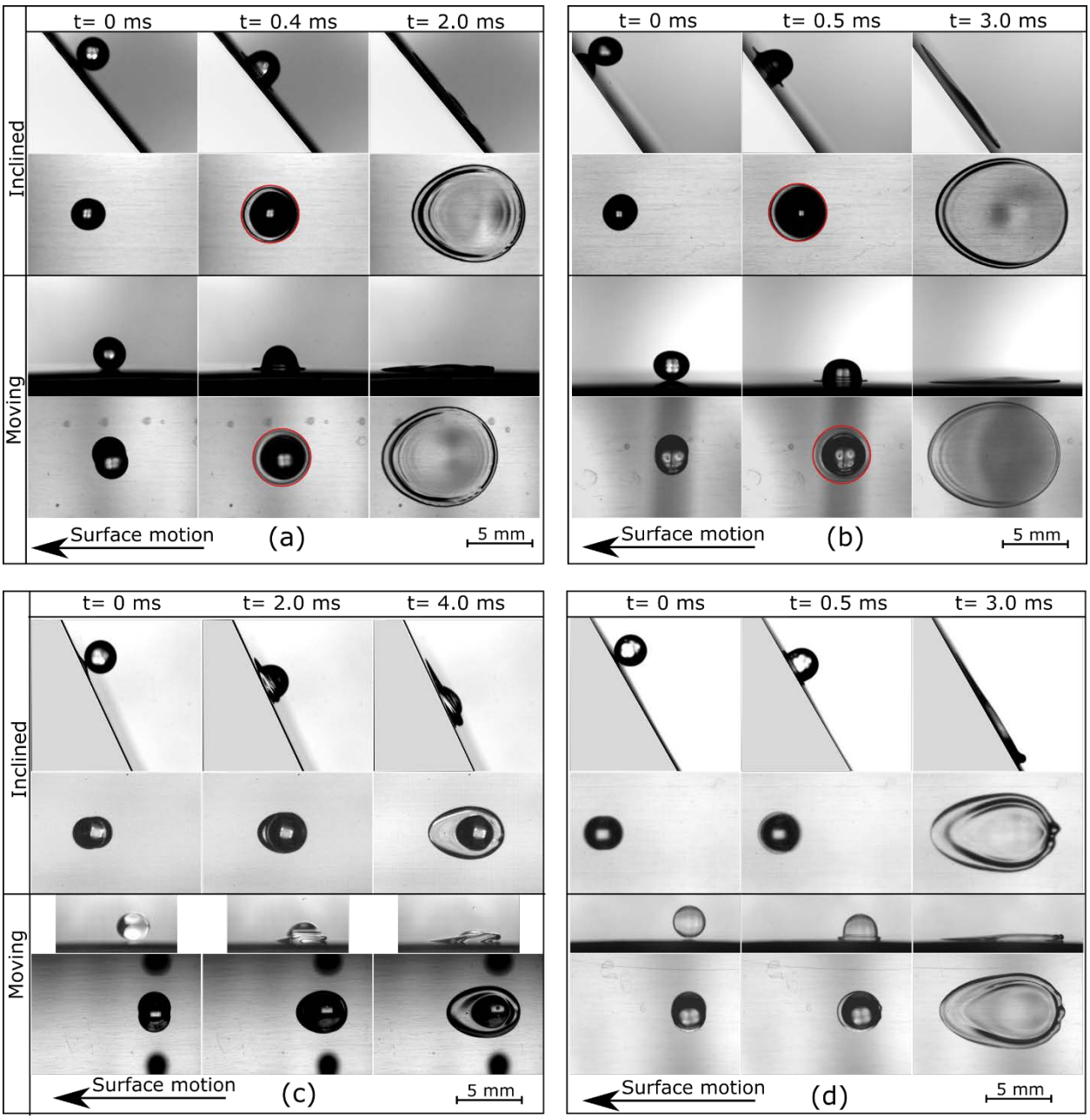

Figure 3.4 showing the spreading of liquids on moving and inclined surfaces at different time intervals on a hydrophilic surface (a) Water D_0=2.5 mm V_n=1.67 m/s V_t= 2.0 m/s; (b) silicone oil (1 cSt) D_0=2.5 mm V_n=1.22 m/s V_t= 1.52 m/s; (c) silicone oil (5 cSt) D_0=2.6 mm V_n=0.38 m/s V_t= 0.81 m/s and (d) 40% Glycerol water D_0=2.5 mm V_n=1.23 m/s V_t= 2.16 m/s.

Figure 3.5 *a* and *b* shows the length and width of the lamella at different time intervals plotted along with their error bars. The data represented here has the highest tangential/surface velocity for which spreading is seen. This means the spreading lamella should experience more resistance from the air moving over the surface. However, from the data, it can be seen that at different time interval, the rate of increase in width for all liquids are same on both inclined and moving surfaces. This means the air movement over the surface do not affect the width of the spreading lamella. Figure 3.5b, shows that the length of the lamella is also similar for both inclined and moving surfaces for all types of liquids, which suggests the gravity do not affect the lamella on inclined surface. (Also see appendix Figure B1 for other velocities). This validates both criteria of our hypothesis for spreading on inclined and moving surfaces.

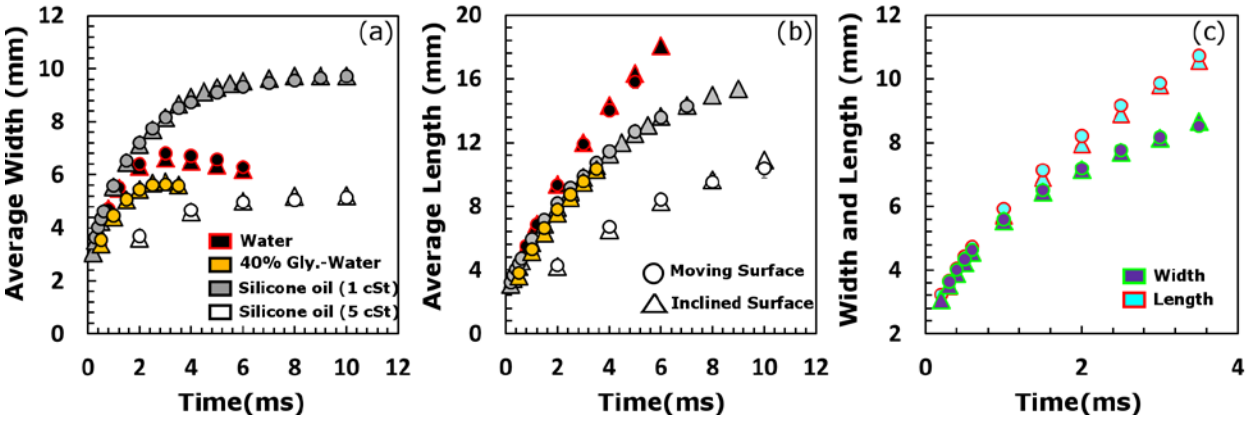

Figure 3.5 Showing the (a) average width; (b) average length on inclined (triangle) and moving surfaces (circle). Water D_0= 2.5 mm V_n= 1.35 m/s V_t= 2.90 m/s (Black), 40% glycerin-water D_0= 2.6 mm V_n= 1.25 m/s V_t= 2.15 m/s (Yellow), Silicone oil (1 cSt) D_0= 2.5 mm V_n= 1.20 m/s V_t= 1.50 m/s (Grey) and silicone oil (5 cSt) D_0= 2.5 mm V_n= 0.50 m/s V_t= 0.90 m/s (Hollow); (c) shows the average width and length of Silicone oil (1 cSt).

3.3.1.1 Applying models from previous literature

Since the first conditions for our spreading hypothesis is met, it is now necessary to see if the position of maximum width is similar for both cases. Therefore, time evolution spreading model for low and high surface tension liquids which was developed for a moving surface (43) can be used to validate the second part of the hypothesis.

The models can predict the shape of the lamella at any given time until t_{max} (i.e. the time a lamella takes to reach the maximum width). The model is based on spreading of liquid on a stationary surface (circular spreading) at different time intervals. In the presence of tangential velocity, they proposed an equation which can predict the lamella spreading (i.e. egg shape or elliptical), depending on few parameters such as surface tension, V_n and V_t.

We use the general spreading model derived in Chapter 2 for water and silicone oil (1 cSt), here, we considered that $V_s = V_t$ (since the same tangential velocity for a given impact condition was used on a moving surface). Figure 3.6 shows the new spreading model applied on our experimental results. On the figure, each circle represents lamella spreading at 0.4 ms intervals. It can be seen that the spreading model can predict the spreading of both low and high surface tension liquids at different time intervals on an inclined surface. This means that the spreading seen on a moving surface is same as the spreading over an inclined surface. Therefore, we can say that the air movement above the surface do not push the maximum width towards downstream region or gravity pulling the maximum width position towards upstream region. Thus we can claim that the spreading on moving and inclined surface are the same for the range of velocities mentioned above.

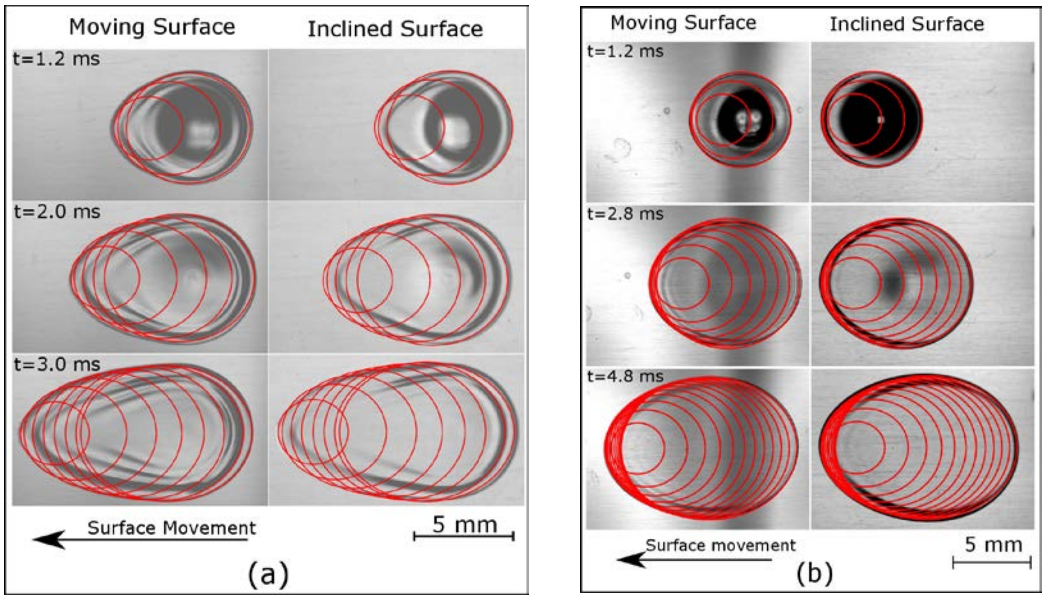

Figure 3.6 Time evolution spreading model applied on (a) water V_n = 1.36 m/s, V_t = 2.9 m/s; and (b) 1 cst silicone oil V_n = 1.24 m/s, V_t = 1.55 m/s.

To summarize, initially, the spreading is dominated by the inertia of the liquid; the inertia creates tangential velocity on an inclined surface which allows the liquid to move down the plane. Spreading is a very fast (around 3-4 ms) phase, and the force of gravity is not strong enough to overcome inertia and viscous forces, hence spreading on an inclined surface is not affected. On a moving surface, we assume that the air velocity above the surface is too low compared to the spreading lamella (which also has an aerodynamic shape), therefore, it cannot affect the spreading on a moving surface. Also on a moving surface, the surface motion cannot change the spreading lamella because the viscous boundary layer thickness ($\sqrt{\nu t}$) during the spreading phase is too low compared to the rim which can affect the rim. Hence, the spreading is similar for both conditions.

3.3.2 Splashing

As the normal velocity and/or the tangential velocity of the droplet was increased, the spreading changes to azimuthal splashing or all around splashing. There are two types of azimuthal and two types of all-around splashing seen on both inclined and moving surfaces. The types of splashes seen moving and inclined surfaces are as follows:

1. Spreading-Prompt splash: Here the downstream region of the droplet spreads while some tiny droplets are generated near the upstream region (Figure 3.7a).
2. Spreading-Corona splash: The lamella in the upstream region lifts off from the surface and droplet detach, while the downstream region spreads (Figure 3.7b).

Both types of splashing take place within a limited azimuthal angle.

3. Prompt-Corona splash: For this case, tiny droplets were generated near the advancing contact line at the downstream region, and lifting off of the lamella was seen at the upstream region (Figure 3.7 c).
4. Asymmetric-Corona splash: All-around corona splash was seen for both upstream and downstream regions (Figure 3.7 d).

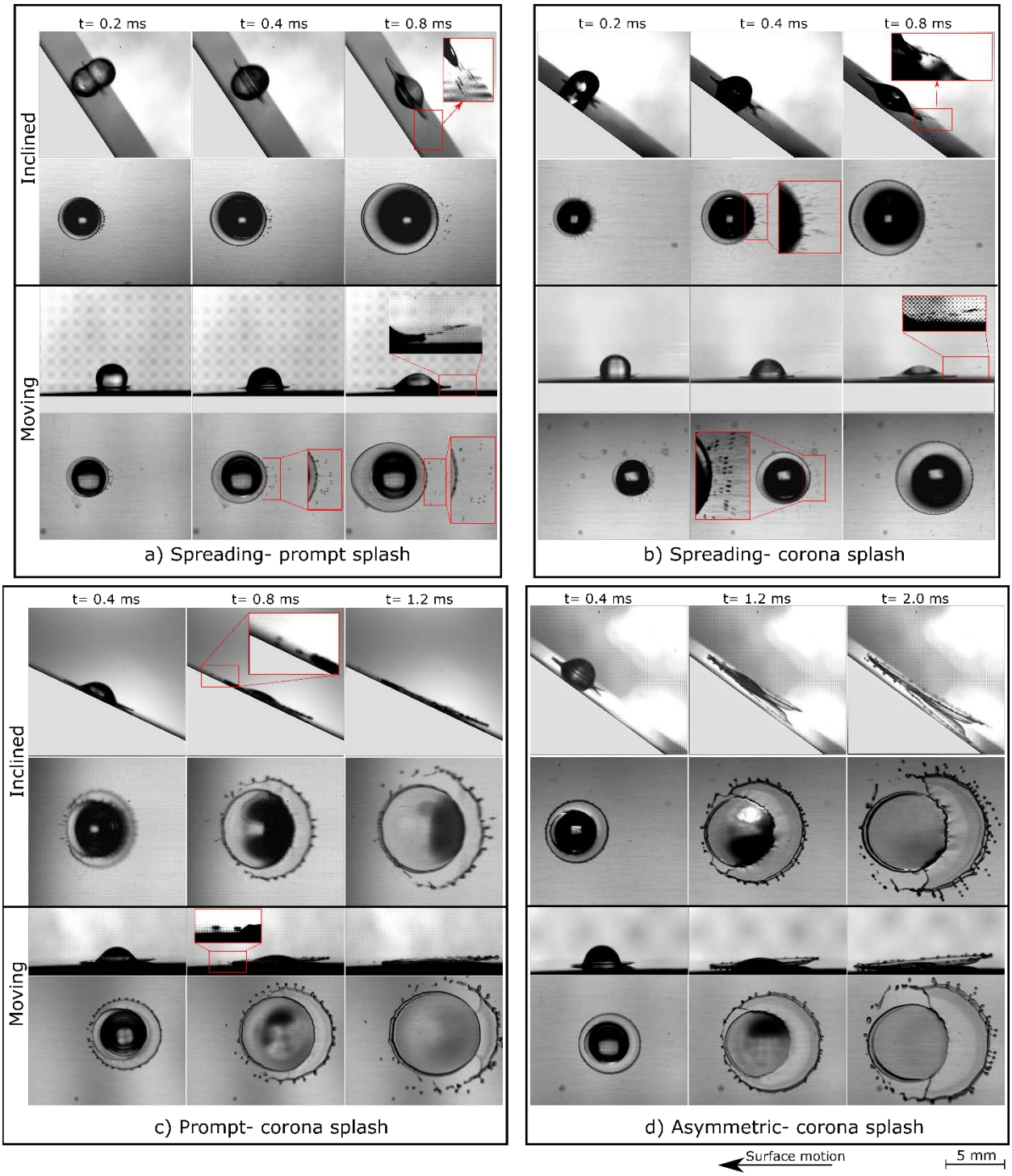

Figure 3.7 Side and overhead views of different types of splashes on inclined and moving surfaces at different time intervals: (a) 1 cst silicone oil V_n =1.68 m/s V_t = 2.38 m/s; (b) 1 cst silicone oil V_n = 2.00 m/s V_t = 1.42 m/s; (c) 40% Glycerol water V_n = 2.90 m/s V_t = 1.36 m/s; (d) 5 cst silicone oil V_n = 2.00 m/s V_t = 1.36 m/s.

The change of spreading to different stages of splashing was seen for all types of liquids except water (for water the tangential velocity was not sufficiently high enough on inclined surfaces for a splash to occur). However, both azimuthal and all-around splash was seen for water for a moving surface at higher V_t (44).

Splashing threshold for 40% glycerol-water, silicone oil 1 and 5 cSt can be seen on Figure 3.8. On the figure the solid line represents the region where drop impact outcome changed. Results shows that when the surface velocity is increased, spreading changes to azimuthal splashing (see V_n= 1.6 m/s and V_t= 2.4 m/s for 1 cSt silicone oil). Azimuthal splashing was seen for all three liquids on both systems. Our experimental results show that the azimuthal angle for a given drop impact conditions is the same for both moving and oblique surfaces, (for details see next section).

For all liquids an increase in normal velocity changes an azimuthal splashing to all-around splashing. Our experimental results show the same type of all-around splashing on inclined and moving surfaces. The following discussion validates our first hypothesis for splashing (i.e the behavior should be similar for both surfaces).

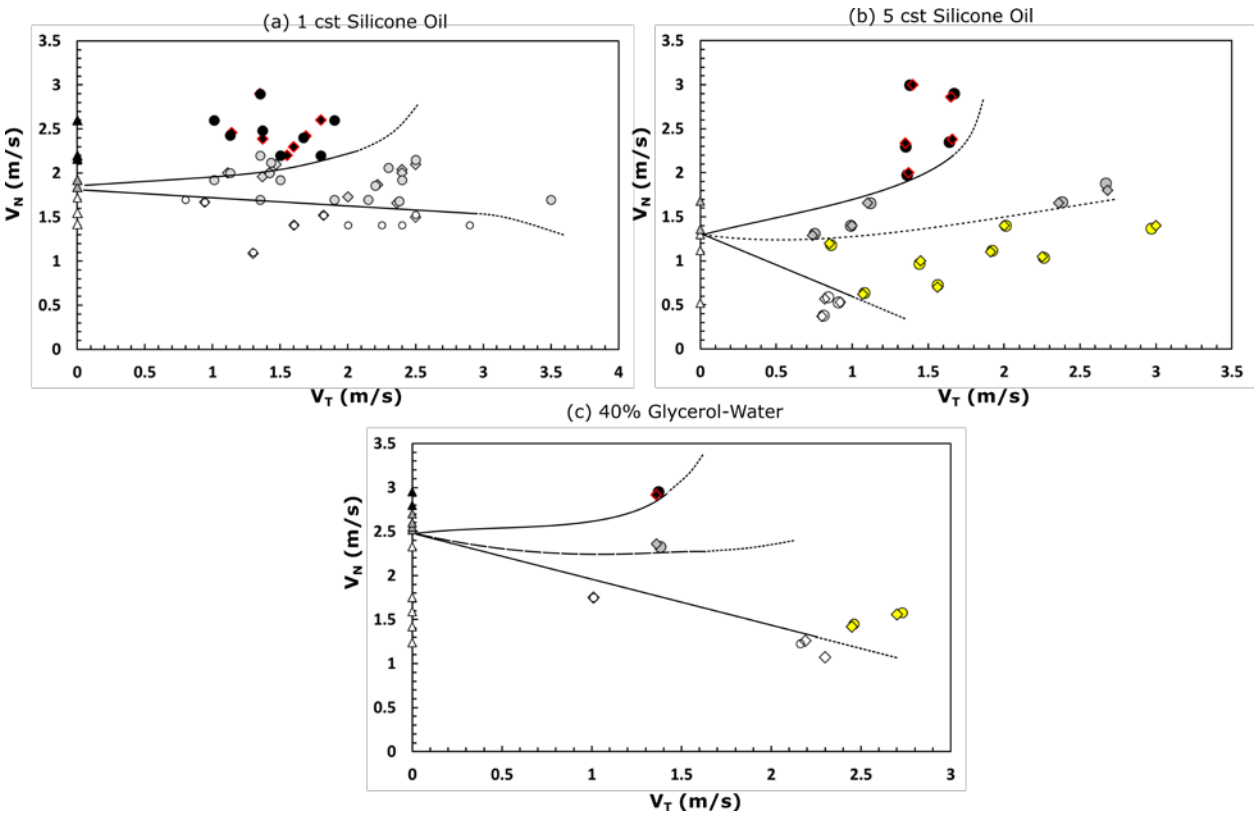

Figure 3.8 Splashing threshold for Silicone oil (1 and 5 cSt) and 40% glycerol-water on stationary (triangle), inclined (diamond) and moving surfaces (circle). Hollow symbols represent spreading, solid grey symbol represents azimuthal splashing, solid black represents all-round splashing and solid-yellow represents new splashing for high viscous liquids. The solid and dashed line are drawn for better visualization of the splashing threshold.

3.3.2.1. Similarities in splashing

From literature (44), azimuthal splash can take place at different extents (i.e. various φ values). The value of φ can vary rapidly when there is a small change in normal velocity or tangential velocity (44). During azimuthal splashing, if the normal velocity is low, the relative velocity between the surface and the lamella in the upstream region is high which enhances tiny droplets to come out of the lamella. On the other hand, if the droplet has a higher normal velocity, the relative velocity between the surface and downstream lamella is low which suppress the splashing at downstream region. Figure 3.9 shows the

azimuthal splashing angles for silicone oil (1 and 5 cSt). For both liquids, the azimuthal splashing can be seen right after impact. For both liquids measurements for different conditions showed that the azimuthal splashing angles on both surfaces are almost similar as the error overlaps each other. This means the air flow over the moving surface do not affect the splashing. Hence our second hypothesis is validated and we can conclude that drop impact on both inclined and moving surfaces are the same for the given drop impact conditions.

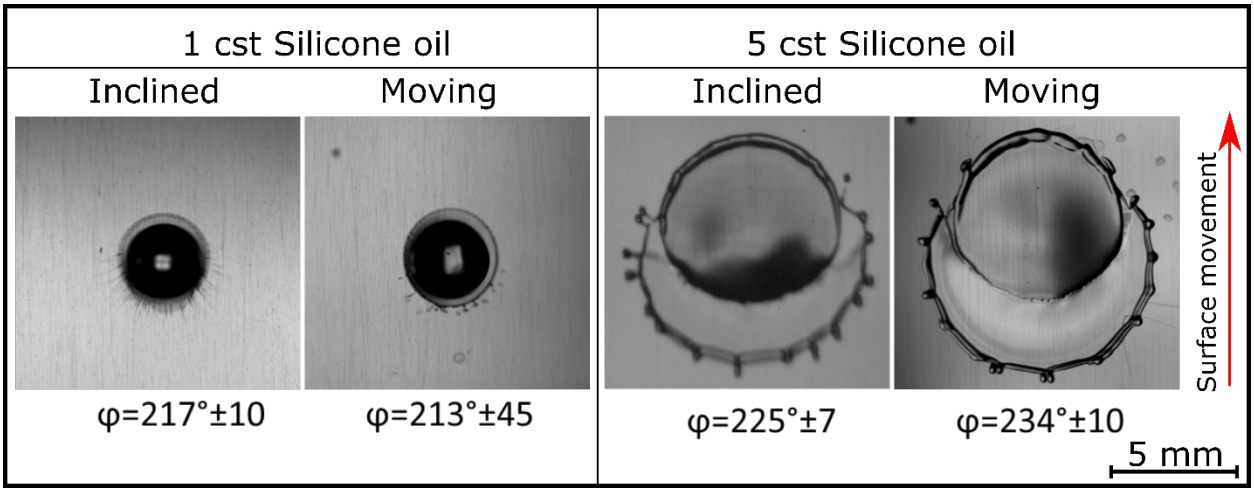

Figure 3.9 Azimuthal splashing angle for 1 cSt silicone oil (Inclined: V_n=2.0 m/s, V_t= 1.42 m/s, moving: V_n=1.99 m/s, V_s= 1.42 m/s) and 5 cSt silicone oil (Inclined: V_n=1.66 m/s, V_t= 1.10 m/s, moving: V_n=1.66 m/s, V_s= 1.12 m/s).

3.3.3 New observation

For high viscous liquids silicone oil (5 cSt) and 40% glycerol-water an unusual type of splashing was observed for both inclined and moving surfaces (see Figure 3.10). This was pointed out on the splashing threshold graph on Figure 3.8 with solid-yellow data points. The phenomenon is similar to a rebounding on a stationary surface, where the

energy in the recoiling phase allows the liquid to jump off from the surface. However, in presence of tangential velocity a split-rebounding is taking place for the condition.

Right after impact the droplet starts to spread slowly due to low V_n, while, kinetic energy from the liquid pushes the liquid (at upstream region) against the tangential velocity. The resultant velocity creates a shear force, which eventually forces the liquid to rip from the lamella. The behavior is similar to a partial rebounding on a stationary surface.

The new type of splash is seen when the normal velocity of the droplet is very low and the surface velocity is high. For higher normal velocity, the split splash changes to azimuthal splashing, which was seen for other liquids.

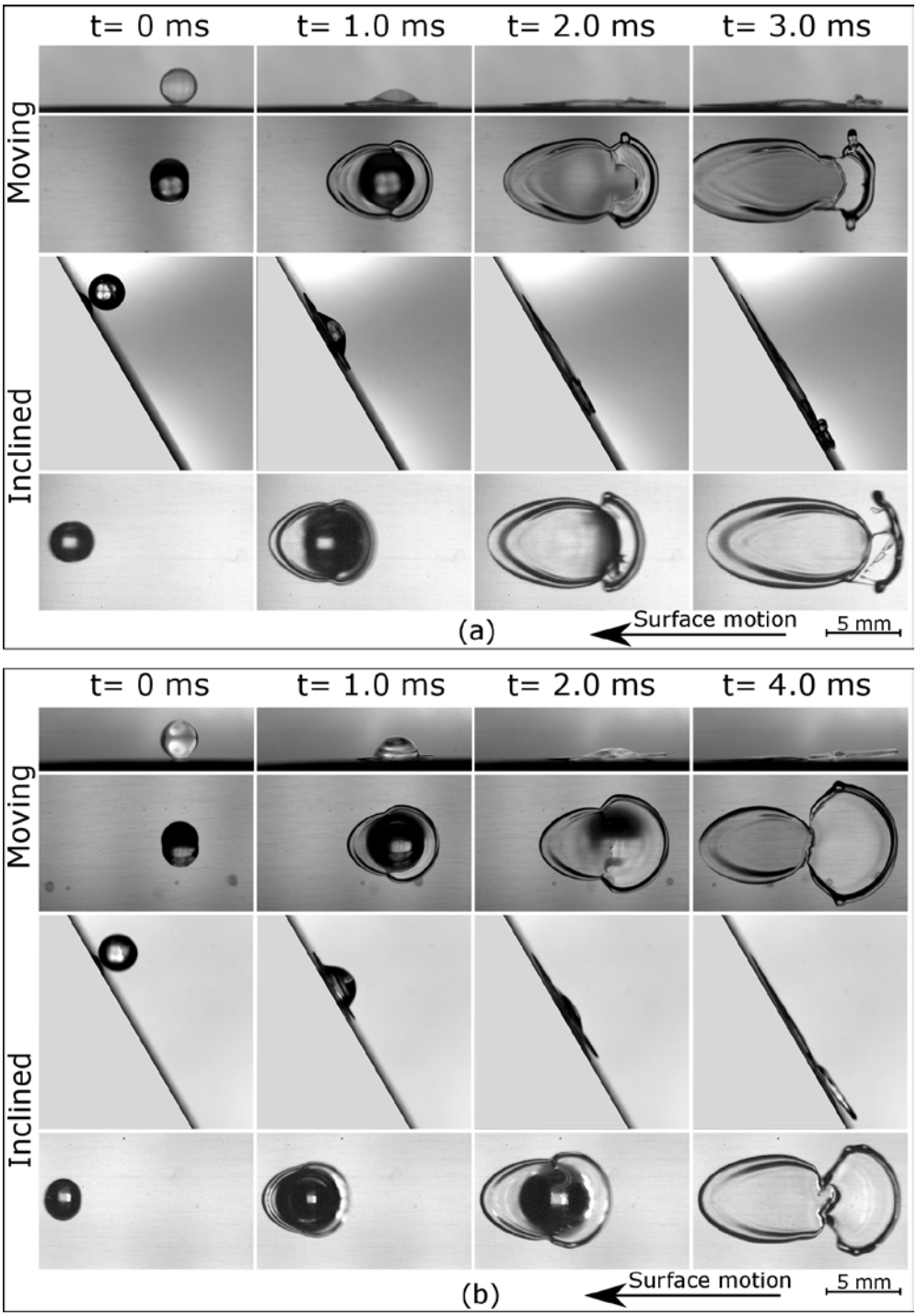

Figure 3.10 Showing split splash on inclined and moving surfaces for viscous liquids (a) 40% glycerol-water, V_n = 1.58 m/s V_t = 2.73 m/s; (b) 5 cst silicone oil at V_n = 1.10 m/s V_t = 1.91 m/s.

Our analysis in this chapter has shown that droplet spreading and splashing are same on both inclined and moving surfaces. Droplet impact on inclined or on moving surface is widely seen in the industry, it is seen on inkjet printing where the surface is moving or in painting industry where the surface can be inclined or moving. Therefore, it is possible for one to design a setup with inclined surface to reproduce similar outcome of a moving surface or vice versa.

Chapter 4

Conclusion and Future works

4.1 Conclusions

In this thesis, for objective 1, we have investigated the spreading behavior for low surface tension liquids on a moving surface. We have used results from previous literature and experimented with water, ethanol, silicone oil to find how low surface tension liquids spread differently compared to high surface tension liquids both on stationary and on moving surfaces. We observed that on a moving surface the position of the maximum width shifts to the center of the lamella, and the shifting increases with surface velocity for low surface tension liquids, this behavior was not seen of high surface tension liquids. For objective 2, we have developed a new spreading model which is a function of time, surface tension, normal and tangential velocity which can predict the spreading of both high and low surface tension liquids with low viscosity on a moving surface.

For objective 3, we have performed systematic experiments on inclined and moving surface to observe the drop impacting behavior. We have discussed how a drop behaves on an oblique and moving surface. Our experimental results in chapter 3 showed that the spreading of liquid on both surfaces are the same. A conclusive outcome was seen when we verified our experimental results for inclined surface with the model, which was developed for moving surfaces. For objective 4, It was noticed that the splashing behavior for both conditions are also same at any given conditions, moreover the splashing angles were also similar to one other. From all our results we finally concluded that drop impact for the conditions discussed here in this thesis is same for dry hydrophilic inclined and moving surfaces.

4.2 Possible Future work

In this this thesis we have provided experimental results for drop impacting on a moving and inclined surfaces. Based on our insight to this topic there are few future works that can be suggested.

In chapter 2 we have discussed about the spreading of low surface tension liquids on a moving surface. A numerical study is suggested to understand how the liquid behaves upon impacting on a moving surface. A numerical study on low surface tension liquids can also give better understanding on how the viscous boundary layer thickness effect the spreading of low and high surface tension liquids on a moving surface.

The spreading model we developed can only work with low viscous (1-4 cst) liquids. However, high viscous liquids spread differently compared to low viscous liquids. Therefore, we suggest to develop a spreading model which can predict the spreading of high viscous liquids. One can also look into the effect of drop impacting behavior of high viscous liquids onto moving surface as this field has not been investigated before. As the spreading for the liquids will be viscous dominated so it will be interesting to see how tangential velocity affects the spreading. We can claim this because our results for 5 cst silicone oil shown different behavior, therefore we think high viscous liquids can also show different splashing behavior upon presence of tangential velocity.

Due to limitations in velocity for inclined surfaces we have not investigated the effect of very high tangential velocity on a moving surface. Therefore, one can investigate how high tangential velocities effect the later part of spreading stage on moving surface, this will help in the painting industry to understand how the paint settles down when sprayed at very high velocity.

Bibliography

1. Worthington AM. XXVIII. On the forms assumed by drops of liquids falling vertically on a horizontal plate. Proc R Soc Lond. 1877 Jan 1;25(171–178):261–72.

2. Minemawari H, Yamada T, Matsui H, Tsutsumi J, Haas S, Chiba R, et al. Inkjet printing of single-crystal films. Nature. 2011 Jul 13;475(7356):364.

3. Jang D, Kim D, Moon J. Influence of Fluid Physical Properties on Ink-Jet Printability. Langmuir. 2009 Mar 3;25(5):2629–35.

4. Ikegawa M, Azuma H. Droplet Behaviors on Substrates in Thin-Film Formation Using Ink-Jet Printing. JSME Int J Ser B Fluids Therm Eng. 2004;47(3):490–6.

5. Le HP. Progress and Trends in Ink-jet Printing Technology. 1999;14.

6. Hansen H. Method for spray-coating medical devices [Internet]. US6669980B2, 2003 [cited 2018 Jun 26]. Available from: https://patents.google.com/patent/US6669980B2/en

7. Huang J, Yuan Z, Gao S, Liao J, Eslamian M. Understanding Spray Coating Process: Visual Observation of Impingement of Multiple Droplets on a Substrate. J Shanghai Jiaotong Univ Sci. 2018 Feb 1;23(1):97–105.

8. Srikar R, Gambaryan-Roisman T, Steffes C, Stephan P, Tropea C, Yarin AL. Nanofiber coating of surfaces for intensification of drop or spray impact cooling. Int J Heat Mass Transf. 2009 Dec 1;52(25):5814–26.

9. Pasandideh-Fard M, Pershin V, Chandra S, Mostaghimi J. Splat Shapes in a Thermal Spray Coating Process: Simulations and Experiments. J Therm Spray Technol. 2002 Jun 1;11(2):206–17.

10. Wirth W, Storp S, Jacobsen W. Mechanisms controlling leaf retention of agricultural spray solutions. Pestic Sci. 1991 Jan 1;33(4):411–20.

11. Massinon M, De Cock N, Forster WA, Nairn JJ, McCue SW, Zabkiewicz JA, et al. Spray droplet impaction outcomes for different plant species and spray formulations. Crop Prot. 2017 Sep 1;99:65–75.

12. Butler Ellis MC, Tuck CR, Miller PCH. How surface tension of surfactant solutions influences the characteristics of sprays produced by hydraulic nozzles used for pesticide application. Colloids Surf Physicochem Eng Asp. 2001 May 31;180(3):267–76.

13. Rein M. Phenomena of liquid drop impact on solid and liquid surfaces. Fluid Dyn Res. 1993 Aug 1;12(2):61–93.

14. Yarin AL. DROP IMPACT DYNAMICS: Splashing, Spreading, Receding, Bouncing…. Annu Rev Fluid Mech. 2006;38(1):159–92.

15. Yarin AL, Weiss DA. Impact of drops on solid surfaces: self-similar capillary waves, and splashing as a new type of kinematic discontinuity. J Fluid Mech. 1995 Jan;283:141–73.

16. Rozhkov A, Prunet-Foch B, Vignes-Adler M. Impact of water drops on small targets. Phys Fluids. 2002 Sep 5;14(10):3485–501.

17. Rioboo R, Tropea C, Marengo M. OUTCOMES FROM A DROP IMPACT ON SOLID SURFACES. At Sprays. 2001;11(2):12.

18. Liu J, Vu H, Yoon SS, Jepsen RA, Aguilar G. SPLASHING PHENOMENA DURING LIQUID DROPLET IMPACT. At Sprays [Internet]. 2010 [cited 2017 Jan 5];20(4). Available from: http://www.dl.begellhouse.com/journals/6a7c7e10642258cc,454ec32d683e6c1b,074a6ae34cf70683.html

19. Prosperetti A, Oguz HN. The Impact of Drops on Liquid Surfaces and the Underwater Noise of Rain. Annu Rev Fluid Mech. 1993 Jan 1;25(1):577–602.

20. Celata GP, Cumo M, Mariani A, Zummo G. Visualization of the impact of water drops on a hot surface: effect of drop velocity and surface inclination. Heat Mass Transf. 2006 Aug 1;42(10):885.

21. Wal RLV, Berger GM, Mozes SD. The splash/non-splash boundary upon a dry surface and thin fluid film. Exp Fluids. 2006 Jan 1;40(1):53–9.

22. Xu F, Jensen OE. Drop spreading with random viscosity. Proc R Soc A. 2016 Oct 1;472(2194):20160270.

23. Reznik SN, Yarin AL. Spreading of a viscous drop due to gravity and capillarity on a horizontal or an inclined dry wall. Phys Fluids. 2001 Dec 20;14(1):118–32.

24. Bartolo D, Josserand C, Bonn D. Retraction dynamics of aqueous drops upon impact on non-wetting surfaces. J Fluid Mech. 2005 Dec;545:329–38.

25. Xu L. Liquid drop splashing on smooth, rough and textured surfaces. Phys Rev E [Internet]. 2007 May 31 [cited 2018 Jun 24];75(5). Available from: http://arxiv.org/abs/physics/0702080

26. Marengo M, Antonini C, Roisman IV, Tropea C. Drop collisions with simple and complex surfaces. Curr Opin Colloid Interface Sci. 2011 Aug;16(4):292–302.

27. Bayer IS, Megaridis CM. Contact angle dynamics in droplets impacting on flat surfaces with different wetting characteristics. J Fluid Mech. 2006 Jul;558:415–49.

28. Yokoi K, Vadillo D, Hinch J, Hutchings I. Numerical studies of the influence of the dynamic contact angle on a droplet impacting on a dry surface. Phys Fluids 1994-Present. 2009 Jul 1;21(7):072102.

29. Hao J, Green SI. Splash threshold of a droplet impacting a moving substrate. Phys Fluids. 2017 Jan 1;29(1):012103.

30. Xu L, Zhang WW, Nagel SR. Drop Splashing on a Dry Smooth Surface. Phys Rev Lett. 2005 May 11;94(18):184505.

31. Lee JB, Derome D, Guyer R, Carmeliet J. Modeling the Maximum Spreading of Liquid Droplets Impacting Wetting and Nonwetting Surfaces. Langmuir. 2016 Feb 9;32(5):1299–308.

32. Lee JB, Derome D, Dolatabadi A, Carmeliet J. Energy Budget of Liquid Drop Impact at Maximum Spreading: Numerical Simulations and Experiments. Langmuir. 2016 Feb 9;32(5):1279–88.

33. Ukiwe C, Kwok DY. On the Maximum Spreading Diameter of Impacting Droplets on Well-Prepared Solid Surfaces. Langmuir. 2005 Jan 1;21(2):666–73.

34. Šikalo Š, Marengo M, Tropea C, Ganić EN. Analysis of impact of droplets on horizontal surfaces. Exp Therm Fluid Sci. 2002 Jan 1;25(7):503–10.

35. Bird JC, Tsai SSH, Stone HA. Inclined to splash: triggering and inhibiting a splash with tangential velocity. New J Phys. 2009;11(6):063017.

36. Cui J, Chen X, Wang F, Gong X, Yu Z. Study of liquid droplets impact on dry inclined surface. Asia-Pac J Chem Eng. 2009 Sep 1;4(5):643–8.

37. LeClear S, LeClear J, Abhijeet, Park K-C, Choi W. Drop impact on inclined superhydrophobic surfaces. J Colloid Interface Sci. 2016 Jan 1;461:114–21.

38. Aboud DGK, Kietzig A-M. Splashing Threshold of Oblique Droplet Impacts on Surfaces of Various Wettability. Langmuir. 2015 Sep 15;31(36):10100–11.

39. Antonini C, Villa F, Marengo M. Oblique impacts of water drops onto hydrophobic and superhydrophobic surfaces: outcomes, timing, and rebound maps. Exp Fluids. 2014 Apr 1;55(4):1713.

40. Fujimoto H, Yoshimoto S, Takahashi K, Hama T, Takuda H. Deformation behavior of two droplets successively impinging obliquely on hot solid surface. Exp Therm Fluid Sci. 2017 Feb;81:136–46.

41. Šikalo Š, Tropea C, Ganić EN. Impact of droplets onto inclined surfaces. J Colloid Interface Sci. 2005 Jun 15;286(2):661–9.

42. Chen RH, Wang HW. Effects of tangential speed on low-normal-speed liquid drop impact on a non-wettable solid surface. Exp Fluids. 2005 Oct 1;39(4):754–60.

43. Almohammadi H, Amirfazli A. Asymmetric Spreading of a Drop upon Impact onto a Surface. Langmuir. 2017 Jun 13;33(23):5957–64.

44. Almohammadi H, Amirfazli A. Understanding the drop impact on moving hydrophilic and hydrophobic surfaces. Soft Matter. 2017;13(10):2040–53.

45. Zen T-S, Chou F-C, Ma J-L. Ethanol drop impact on an inclined moving surface. Int Commun Heat Mass Transf. 2010 Oct;37(8):1025–30.

46. Schremb M, Roisman IV, Tropea C. Transient effects in ice nucleation of a water drop impacting onto a cold substrate. Phys Rev E. 2017 Feb 23;95(2):022805.

47. Fathi S, Dickens P, Fouchal F. Regimes of droplet train impact on a moving surface in an additive manufacturing process. J Mater Process Technol. 2010 Feb 1;210(3):550–9.

48. Mundo C, Sommerfeld M, Tropea C. Droplet-wall collisions: Experimental studies of the deformation and breakup process. Int J Multiph Flow. 1995 Apr 1;21(2):151–73.

49. Yeong YH, Burton J, Loth E, Bayer IS. Drop Impact and Rebound Dynamics on an Inclined Superhydrophobic Surface. Langmuir. 2014 Oct 14;30(40):12027–38.

50. Kang BS, Lee DH. On the dynamic behavior of a liquid droplet impacting upon an inclined heated surface. Exp Fluids. 2000;29(4):0380–7.

51. Clanet C, Béguin C, Richard D, Quéré D. Maximal deformation of an impacting drop. J Fluid Mech. 2004 Sep;517:199–208.

52. Tang C, Qin M, Weng X, Zhang X, Zhang P, Li J, et al. Dynamics of droplet impact on solid surface with different roughness. Int J Multiph Flow. 2017 Nov 1;96:56–69.

53. Vaikuntanathan V, Sivakumar D. Maximum Spreading of Liquid Drops Impacting on Groove-Textured Surfaces: Effect of Surface Texture. Langmuir. 2016 Mar 15;32(10):2399–409.

54. Antonini C, Amirfazli A, Marengo M. Drop impact and wettability: From hydrophilic to superhydrophobic surfaces. Phys Fluids 1994-Present. 2012 Oct 1;24(10):102104.

55. Sadek Khattab I, Bandarkar F, Abolghassemi Fakhree MA, Jouyban A. Density, viscosity, and surface tension of water+ ethanol mixtures from 293 to 323K. Korean J Chem Eng. 2012 Jun 1;29.

56. McPherson R. The relationship between the mechanism of formation, microstructure and properties of plasma-sprayed coatings. Thin Solid Films. 1981 Sep 18;83(3):297–310.

57. Cui J, Chen X, Wang F, Gong X, Yu Z. Study of liquid droplets impact on dry inclined surface. Asia-Pac J Chem Eng. 2009 Sep 1;4(5):643–8.

58. Liang G, Guo Y, Shen S, Yu H. A study of a single liquid drop impact on inclined wetted surfaces. Acta Mech. 2014 Dec 1;225(12):3353–63.

59. Shen C, Yu C, Chen Y. Spreading dynamics of droplet on an inclined surface. Theor Comput Fluid Dyn. 2016 Jun 1;30(3):237–52.

60. Xu L. Liquid drop splashing on smooth, rough, and textured surfaces. Phys Rev E. 2007 May 31;75(5):056316.

61. Wal RLV, Berger GM, Mozes SD. The combined influence of a rough surface and thin fluid film upon the splashing threshold and splash dynamics of a droplet impacting onto them. Exp Fluids. 2006 Jan 1;40(1):23–32.

62. Physical Properties of glycerine and its solutions. New York, N.Y.: Glycerine Producer’s Assoc.; 1975.

63. Calculate density and viscosity of glycerol/water mixtures [Internet]. [cited 2018 Jun 17]. Available from: http://www.met.reading.ac.uk/~sws04cdw/viscosity_calc.html

Appendices

Supporting information for chapter 2

A.1 Downstream region moving with surface velocity

On a moving surface, right after impact, the spreading lamella has a higher velocity compared to the surface. But as time progresses, the spreading lamella at the downstream region starts losing its kinetic energy. Figure S1 shows the lamella velocity at the downstream region at initial time for two different drop impact conditions for both water and silicone oil (1 cSt). From the Figure, it can be noticed that the lamella velocity starts to decrease as time progress; however, after a certain time the lamella velocity becomes constant which is equal to the surface velocity. From this information, we can say that the lamella at the downstream region stopped spreading and started moving with the surface velocity.

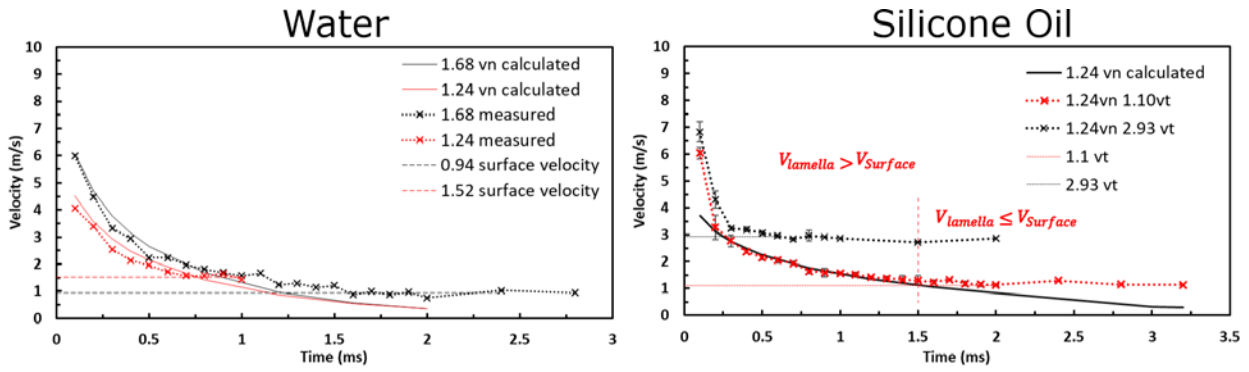

Figure A.1 Shows the lamella velocity of water and silicone plotted against time. the solid line was drawn by computing the lamella velocity using eq. 3. The experimental data are plotted as cross and the horizontal dashed line represents the surface velocity. (a) water V_n=1.68 V_s=1.00 (black); V_n=1.24 V_s= 1.52m/s (Red); (b) Silicone oil V_n=1.24 V_s= 2.93 m/s (black) and V_s= 1.10 m/s (red).

A.2 Stretching of lamella

Stretching and shrinking of lamella was seen for all droplet impact conditions. Figure S2 shows the stretching and shrinking for V_n= 1.5m/s for different surface velocity. Here it can be seen that for both normal velocities the stretching starts around 2.8 ms (see the box in the figure). Also it can be seen that both stretching and shrinking are larger for high surface velocities

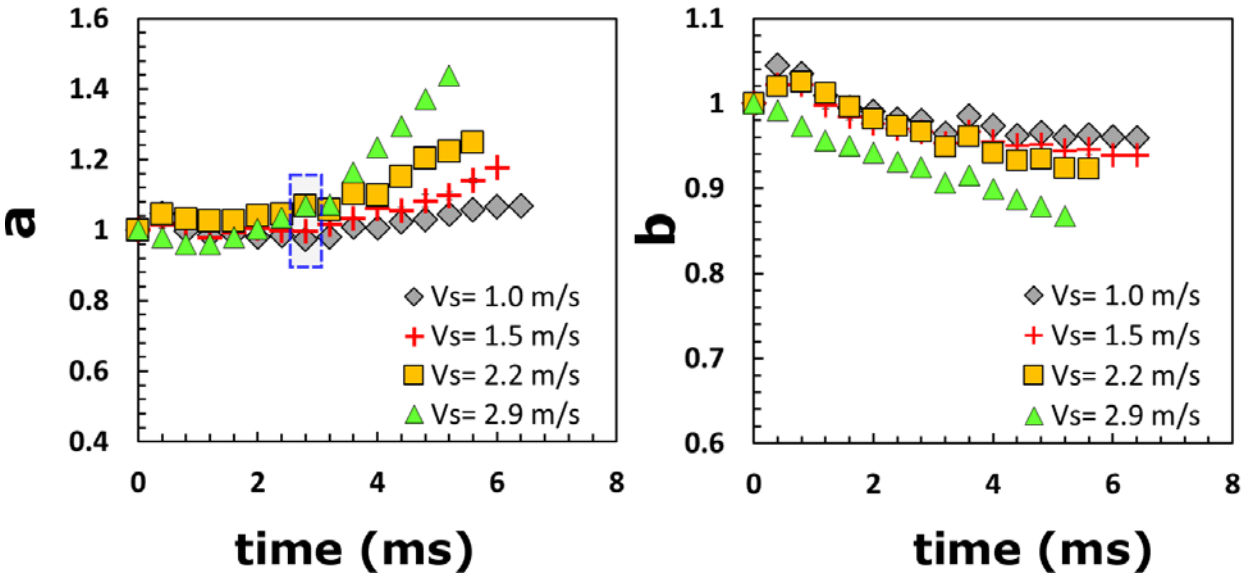

Figure A.2 The stretching of lamella in the direction of motion ***a,*** *and the shrinking of lamella perpendicular to the direction of motion* ***b*** *normalized by r(t) of a stationary surface****,*** *at different time intervals for V_n=1.5 m/s; and four different surface velocities V_s=1.0 m/s (diamond), 1.5 m/s (cross), 2.2 m/s (square). 2.9 m/s (triangle)*

A.3 Stretching factors (a)

The stretching factor ***a,*** was calculated using our experimental data at different drop impact conditions. Based on our observations we have noticed that the shifting factors depends on the following parameters

$$\mathrm{a} = f(t, V_n, V_s)$$

In order to observe how each parameter varies the shifting factor, we have plotted each variable seperately. Figure S3 a-c shows how the maximum widith stretches with each parameter t, V_s and V_n. As it can be seen that for all the parameters, the stretching factors has a positive power relation with time and surface velocity and a negetive power relation with normal velocity. Therefore we suggest the following form:

$$\mathbf{a} = \alpha\beta^{t} {V_n}^{\phi} {V_s}^{d} + e \ ,$$

where *a* to *e* are fitting coefficients. The coefficients were found using the Non-Linear Regression toolbox in SPSS software. α = 0.008, β=1.601, ϕ = -0.619, *d* =1.559 and *e* =1.000, where time is in ms and both V_s, V_n are in m/s. Here, R^2= 0.945 and SSE=0.153.

A.4 Width factor (b)

The width factor **b**, was found in a similar manner as discussed before. Our experimental data showed that the shifting is also dependant on the following parametersV_S

$$\mathrm{b} = f(t, V_n, V_s)$$

Figure S3 *d* to *e* shows the stretching factor with each parameter. As it can be seen that for all the parameters, the shrinking factors forms a power relation with all other independant variables. Therefore we suggest the following form:. Hence, we suggest the following form:

$$\mathbf{b} = f g^{t} {V_n}^{h} {V_s}^{i} + j$$

Here *f*=-0.025, *g*=1.210, *h*=0.292, *i*=0.693 and *j*=1.000, where time is in ms and both V_S, V_N are in m/s. Here, R^2= 0.705 and SSE=1.229.

A.5 Shifting factor (C)

The shifting factor ***C,***was calculated using our experimental data at different drop impact conditions. Based on our observations we have noticed that the shifting factors depends on the following parameters

$$C = f(t, V_n, V_s)$$

As it can be seen that for all the parameters, the shifting factors has a power relation with all independant variables. Therefore we suggest the following form:

$$C = \varepsilon t^{\delta} {V_n}^{\xi} {V_s}^{\tau}$$

Here, ε= 0.096, δ=1.767, ξ= 0.468 and τ= 0.926; where the time is in ms and the value of C is in mm. R^2= 0.992 and SSE= 3.756.

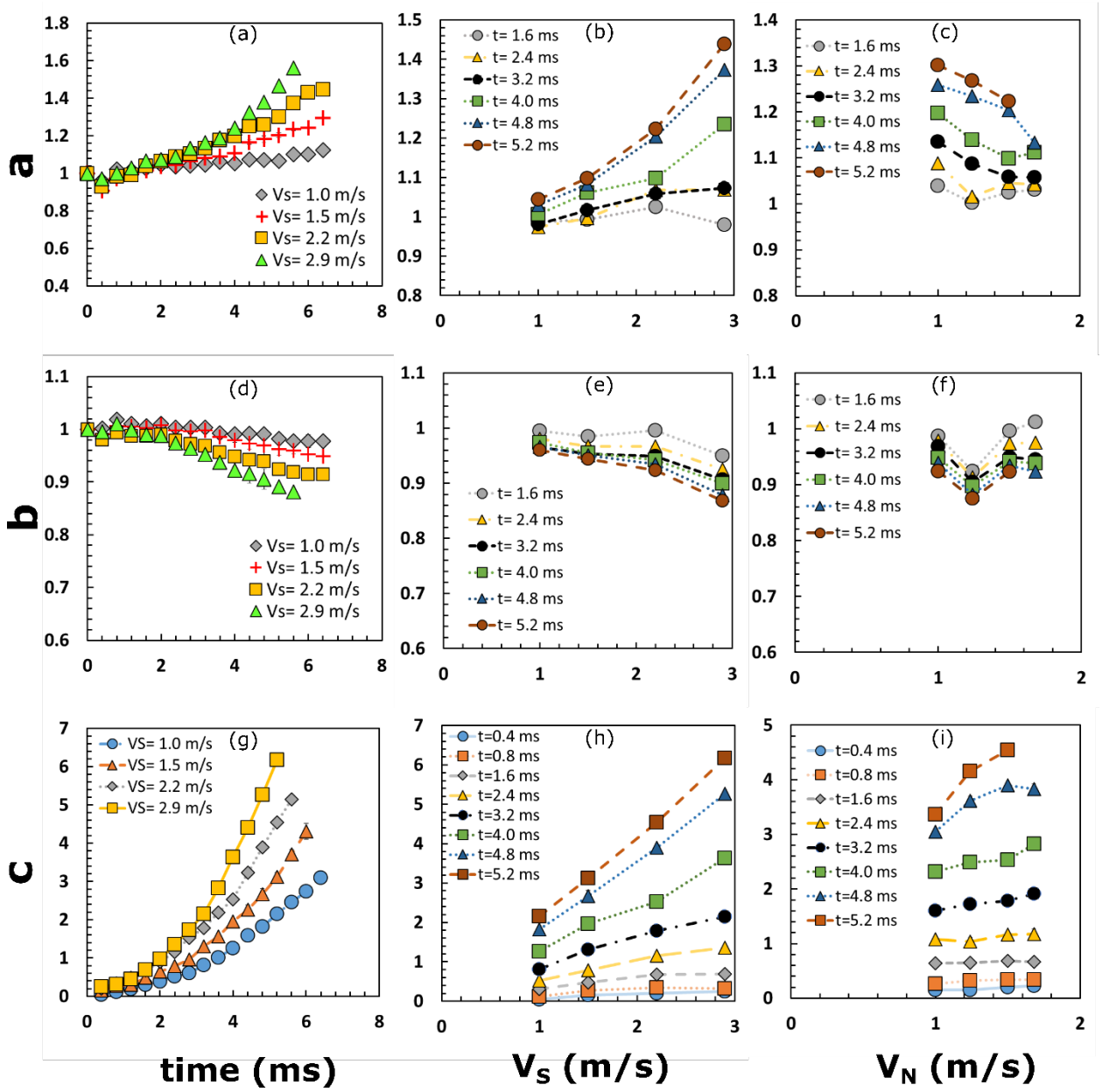

Figure A 3 Shows the stretching factor (a to c), shrinking factor (d to f) and shifting factor (g to i) with respect to time (a, d, g), surface velocity (b, e, h), normal velocity (c, f, i) for the droplet impact conditions (a, d) V_n= 1.0 m/s, (c) V_n= 1.5 m/s, (b, e and f) V_n= 1.5 m/s, (c, f and i) V_s= 2.2 m/s D_0=2.5mm.

Appendix B

B.1

Average width and length were measured for other droplet velocities on inclined and moving surfaces. Figure B1 *a* and *b*, shows our experimental results for all four types of liquid. From this figure it can be seen that spreading of for other droplet impact conditions are also similar for inclined and moving surfaces.

High viscous liquids also spreads radially at initial time right after impact this can be seen in Figure B 1 *c*. From the figure, the length and width of the spreading lamella overlaps until t= 1.0 ms and the plot starts to deviate at t=1.5 ms, which confirms the spreading is radial for high viscous liquids.

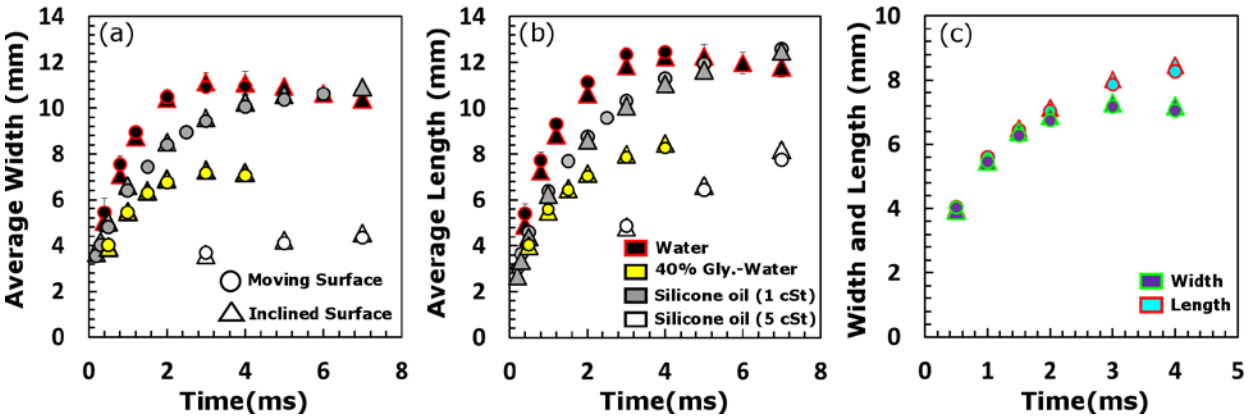

Figure B. 1 Shows the (a) average width; (b) average length on inclined (triangle) and moving surfaces (circle). Water D0= 2.5 mm Vn= 2.88 m/s Vt= 1.36 m/s (Black), 40% glycerin-water D0= 2.6 mm Vn= 1.75 m/s Vt= 1.01 m/s (Yellow), Silicone oil (1 cSt) D0= 2.5 mm Vn= 1.68 m/s Vt= 1.00 m/s (Grey) and silicone oil (5 cSt) D0= 2.5 mm Vn= 0.38 m/s Vt= 0.80 m/s (Hollow); (c) shows the average width and length of 40% glycerin-water Vn= 1.75 m/s Vt= 1.01 m/s.

B2. Azimuthal Splash

Azimuthal splash was also measured for other drop impact conditions for silicone oil (1 and 5 cSt).

The table below shows the azimuthal splashing angles for other drop impact condition.

Table B. 1: Azimuthal splashing angles for silicone oils on inclined and moving surface

liquid	Inclined			Moving		
Silicone oil (1 cSt)	Velocity, m/s		Splashing angle, φ	Velocity		Splashing angle, φ
	Normal	Tangential		Normal	Tangential	
	V_n= 1.96	V_t= 1.13	224° ± 26°	V_n= 1.98	V_t= 1.13	287°± 55°
	V_n= 1.66	V_t= 2.36	97° ± 10°	V_n= 1.68	V_t= 2.38	102°± 12°
	V_n= 2.10	V_t= 1.47	204° ± 23°	V_n= 2.12	V_t= 1.43	214°± 56°
Silicone oil (5 cSt)	V_n= 1.40	V_t= 1.00	234° ± 5°	V_n= 1.40	V_t= 0.99	240°± 4°
	V_n= 1.40	V_t= 2.00	200° ± 9°	V_n= 1.40	V_t= 2.01	202°± 5°
	V_n= 1.66	V_t= 2.36	199° ± 3°	V_n= 1.67	V_t= 2.36	202°± 4°
	V_n= 1.88	V_t= 2.68	219° ± 5°	V_n= 1.88	V_t= 2.67	223°± 10°

Appendix C

C1. Measurement of droplet size

A grid scale was used to measure the droplet size. A grid scale contains small square grids, where each square has a length of 0.25mm. The scale was placed on the focal plane of the lens which gave a sharper image of the grid and few snapshot are taken for use. On the inkscape software, the length of 4 square boxes were measured in pixels which gave the scale for each pixels in millimeter.

The droplet diameter was measured by measuring the length of the spherical droplet in x and y direction, and it was converted to standard unit by using the scale. The procedure was repeated 3 time for different liquids.

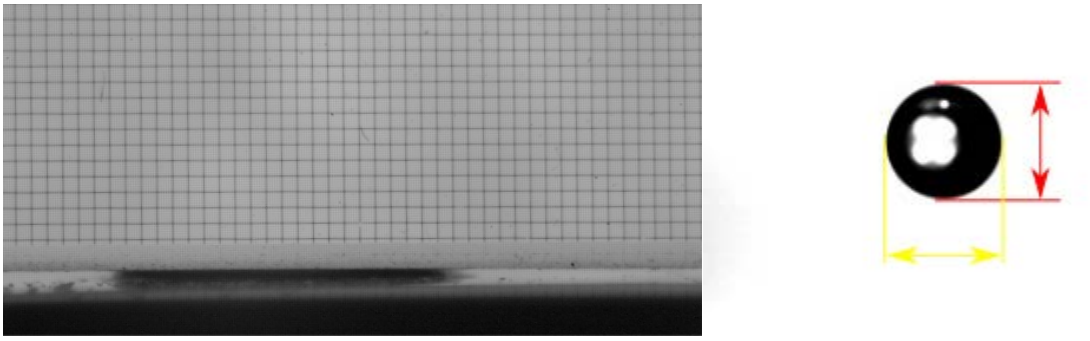

(a) (b)

Figure C. 1 a) shows the grid scale used for measurement; b) shows how droplet diameter was measured for experiments.

C 2. Measurement of velocity

The normal velocity of the droplet was measured by taking snapshot of the video at different time intervals. The position of the droplet from different images were measured using inkscape in pixels which was converted to standard unit. The ratio of distance travelled by a droplet to time gave the velocity of the droplet.

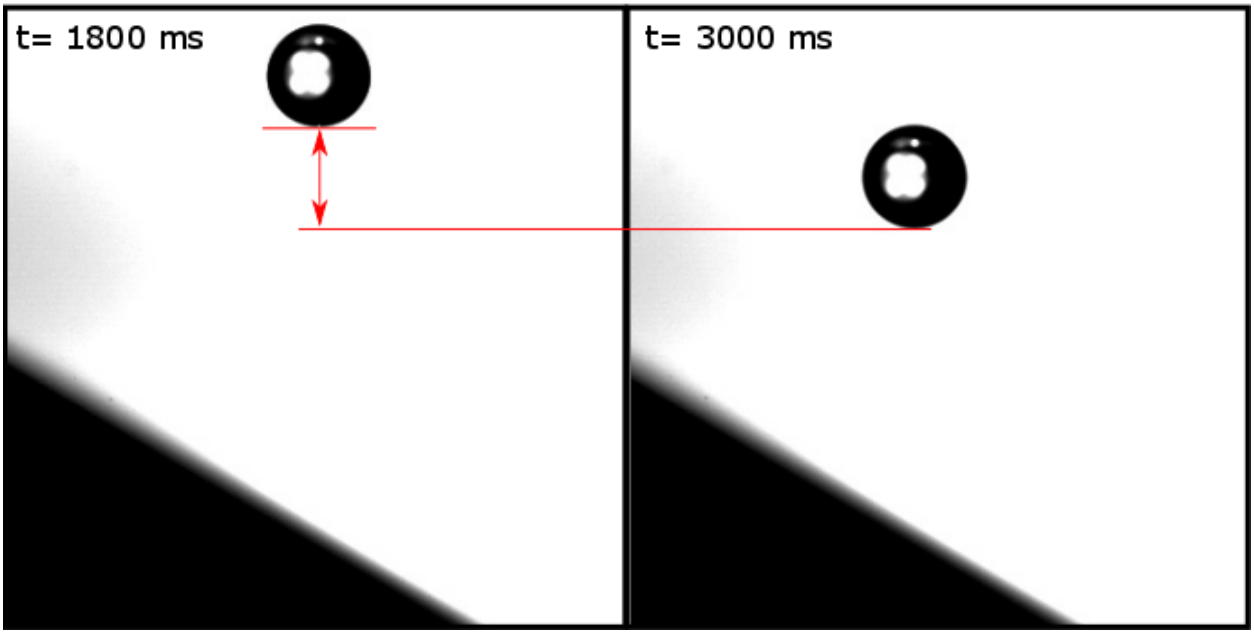

Figure C. 2 Snapshot of droplet impacting on inclined surface at different time intervals used for measuring normal velocity of the droplet.

C 3. Contact angle

Surface wettabilitiy determines if the surface is hydrophilic or hydrophobic, If the advancing contact angle of a droplet is below 90, it is considered hydrophilic; value above 90 is considered hydrophobic surface. The surface wettability was measured using the Kruss Drop Shape Analyzer 100E, which has inbuilt software to measure the contact angles. The advancing and receding contact angles were measured on different places on the surface to get accurate result

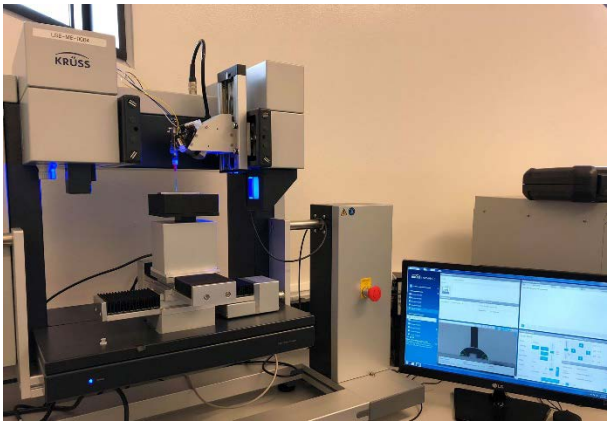

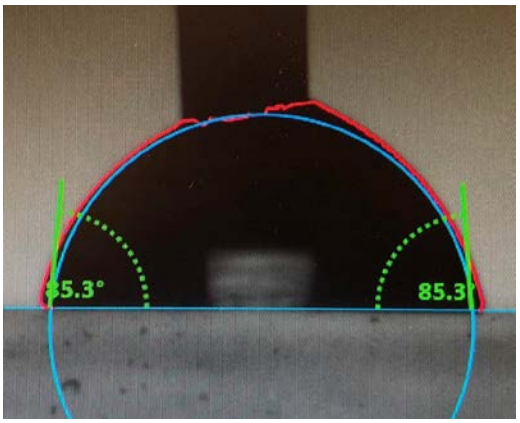

(a) (b)

Figure C. 3 a) showing the Kruss DSA 100E used for measuring droplet contact angles; b) image of contact angle measured on the surface.